

Combined explanations of B -physics anomalies, $(g - 2)_{e,\mu}$ and neutrino masses by scalar leptoquarks

Shao-Long Chen,^{1,2,*} Wen-wen Jiang,^{1,†} and Ze-Kun Liu^{1,‡}

¹*Key Laboratory of Quark and Lepton Physics (MoE) and Institute of Particle Physics,
Central China Normal University, Wuhan 430079, China*

²*Center for High Energy Physics, Peking University, Beijing 100871, China*

We extend the contents of the standard model (SM) by introducing TeV-scale scalar leptoquarks to generate neutrino masses and explain some current observed deviations from the SM predictions, including the anomalous magnetic moments of charged leptons (electron and muon) and B -physics anomalies ($R_{K^{(*)}}$ and $R_{D^{(*)}}$). The model consists of $SU(2)_L$ singlet leptoquark $S_1 \sim (\bar{3}, 1, 1/3)$, doublet leptoquark $\tilde{R}_2 \sim (3, 2, 1/6)$ and triplet leptoquark $S_3 \sim (\bar{3}, 3, 1/3)$. We combine the constraints arising from the low-energy lepton flavor violation, meson decay and mixing observables. We perform a detailed phenomenological analysis and identify the minimized texture of leptoquark Yukawa matrices to accommodate a unified explanation of the anomalies and neutrino oscillation data.

* E-mail: chensl@mail.ccnu.edu.cn

† E-Mail: wwjiang@mails.ccnu.edu.cn

‡ E-mail: zekunliu@mails.ccnu.edu.cn

I. INTRODUCTION

The neutrino oscillation experiments have firmly established that neutrinos are massive and have non-trivial mixing between different generations [1–4]. The experiments also indicate that the neutrino masses are much smaller than that of charged fermions, which suggests that neutrinos may have specific sources of mass generation. In the recent decades, a plethora of models have been proposed to explain the neutrino mass and the natural way is the so called seesaw mechanism [5]. Type-I seesaw model [6–10] provides neutrino masses at the tree-level by extending the particle content of the SM with three $SU(2)_L$ -singlet right-handed neutrino fields, while type-II [10–12] and type-III [13] models introduce $SU(2)_L$ -triplet scalar and $SU(2)_L$ -triplet fermions, respectively. Beyond tree level, the tiny neutrino masses could radiatively originate from loop levels [14–18].

Extending the SM to include the source of the origin of neutrino mass and mixing brings new physics, especially to the flavor sector. The intensity frontier precision measurements may pin down the possible connections between neutrino physics and flavor physics. Such as the anomalous magnetic moments of electron and muon, there are long-standing discrepancies between the theoretical predictions and measured values [19–41]. The anomalies also include the ratios $R_{K^{(*)}}$ and $R_{D^{(*)}}$ in B -decays, pointing towards the lepton flavor universality violation, measured by BaBar [42, 43], Belle [44–46] and LHCb [47–51] collaborations. In this work, we propose a model with scalar leptoquarks to provide a common explanation of neutrino mass and these flavor anomalies.

Leptoquarks (LQs) have been introduced in many new physics models beyond the SM and are very popular to explain B -physics anomalies with one or more leptoquark states [52–54]. The unified solution to both $R_{K^{(*)}}$ and $R_{D^{(*)}}$ anomalies seems rule out single scalar leptoquark models [55]. Among the scalar leptoquarks, triplet $S_3 \sim (\bar{3}, 3, 1/3)$ can accommodate the $R_{K^{(*)}}$ anomalies, while the $R_{D^{(*)}}$ anomalies can be resolved by introducing either a singlet $S_1 \sim (\bar{3}, 1, 1/3)$ or a doublet $R_2 \sim (3, 2, 7/6)$ leptoquark. The double leptoquarks models were proposed to explain both $R_{K^{(*)}}$ and $R_{D^{(*)}}$ anomalies, involving S_1 and S_3 combination [56–61] or R_2 and S_3 combination [62–64]. Extending with leptoquarks will give contribution to the anomalous magnetic moment of charged lepton at one-loop level and the no-chiral scalar leptoquarks S_1 or R_2 , which have both left-chiral and right-chiral couplings, can provide good explanations to the a_μ and a_e deviations [65, 66] simultaneously. The mixing between different type leptoquarks can also generate non-trivial Majorana neutrino mass terms at one-loop level. The minimal model to generate neutrino mass by the scalar leptoquark mixing requires a pair of leptoquarks and the possible combinations are $S_1 - \tilde{R}_2(3, 2, 1/6)$, $S_3 - \tilde{R}_2$ and $S_3 - R_2$ [67–71]. Motivated by the leptoquark abundant phenomenologies, we attempt to extend the SM contents by scalar leptoquarks to generate neutrino mass and explain the flavor anomalies mentioned above.

This paper is organized as follow: In Section II, we briefly introduce the model set-up and the neutrino mass generation mechanism. In Section III, we show how to explain the

flavor anomalies in the model, including $R_{K^{(*)}}$, $R_{D^{(*)}}$, a_μ and a_e . We discuss the observables constraints on the leptoquark couplings in Section IV and then we perform a detailed analysis of model parameter space and identify two benchmark points in Section V and we conclude in the final section.

II. THE MODEL AND NEUTRINO MASS GENERATION

A. The model

In addition to the SM fields, we introduce three scalar leptoquarks, including an $SU(2)_L$ singlet $S_1 \sim (\bar{3}, 1, 1/3)$, a doublet $\tilde{R}_2 \sim (3, 2, 1/6)$ and a triplet $S_3 \sim (\bar{3}, 3, 1/3)$. The scalar leptoquarks are denoted as

$$\begin{aligned} S_1(\bar{3}, 1, 1/3) &= S_1^{1/3}, \quad \tilde{R}_2(3, 2, 1/6) = (\tilde{R}_2^{2/3}, \tilde{R}_2^{-1/3})^T, \\ S_3(\bar{3}, 3, 1/3) &= \tau^i S_3^i = \begin{pmatrix} S_3^{1/3} & \sqrt{2} S_3^{4/3} \\ \sqrt{2} S_3^{-2/3} & -S_3^{1/3} \end{pmatrix}, \end{aligned} \quad (1)$$

where τ^i ($i = 1, 2, 3$) are the Pauli matrices and we define $S_3^{4/3} = (S_3^1 - iS_3^2)/\sqrt{2}$, $S_3^{-2/3} = (S_3^1 + iS_3^2)/\sqrt{2}$ and $S_3^3 = S_3^3$. The corresponding Yukawa terms that describe the interactions between leptoquarks and fermions are given by

$$\begin{aligned} \mathcal{L}_Y &= -y_{1R}^{ij} \bar{u}_R^{iC} e_R^j S_1 - y_{1L}^{ij} \bar{Q}_L^{iC} i\tau^2 L_L^j S_1 - y_{2L}^{ij} \bar{d}_R^i \tilde{R}_2^T i\tau^2 L_L^j \\ &\quad - y_{3L}^{ij} \bar{Q}_L^{iC} i\tau^2 S_3 L_L^j + \text{h.c.}, \end{aligned} \quad (2)$$

where Q and L denote the $SU(2)_L$ doublet left-handed quarks and leptons, u_R , d_R and e_R denote the $SU(2)_L$ singlet right-handed up-type quarks, down-type quarks and charged leptons, respectively. All fields in Eq. (2) are represented in the flavor basis. For phenomenological analysis, it is more convenient that we re-parametrize the couplings in the fermion mass basis. The Yukawa coupling terms are then rewritten in the mass basis of fermions as the following form,

$$\begin{aligned} \mathcal{L}_Y &= -y_{1R}^{ij} \bar{u}_R^{iC} e_R^j S_1^{1/3} + (V^T y_{1L})^{ij} \bar{d}_L^{iC} \nu_L^j S_1^{1/3} - y_{1L}^{ij} \bar{u}_L^{iC} e_L^j S_1^{1/3} + y_{2L}^{ij} \bar{d}_R^i \nu_L^j \tilde{R}_2^{-1/3} \\ &\quad - y_{2L}^{ij} \bar{d}_R^i e_L^j \tilde{R}_2^{2/3} + (V^T y_{3L})^{ij} \bar{d}_L^{iC} \nu_L^j S_3^{1/3} + \sqrt{2}(V^T y_{3L})^{ij} \bar{d}_L^{iC} e_L^j S_3^{4/3} \\ &\quad - \sqrt{2} y_{3L}^{ij} \bar{u}_L^{iC} \nu_L^j S_3^{-2/3} + y_{3L}^{ij} \bar{u}_L^{iC} e_L^j S_3^{1/3} + \text{h.c.} \end{aligned} \quad (3)$$

where V is the CKM matrix. Since in our analysis of $(g-2)_{e,\mu}$ and B -physics anomalies, the choice of neutrino mass or flavor basis has negligible effect, the neutrino states in the above equation are kept in flavor basis.

The renormalizable and gauge invariant scalar potential involving H , S_1 , \tilde{R}_2 and S_3 is described by

$$V \supset m_H^2 H^\dagger H + m_1^2 S_1^\dagger S_1 + m_2^2 \tilde{R}_2^\dagger \tilde{R}_2 + \frac{1}{2} m_3^2 \text{Tr}(S_3^\dagger S_3) + \lambda_H (H^\dagger H)^2 + \lambda_1 (S_1^\dagger S_1)^2$$

$$\begin{aligned}
& + \lambda_2 \left(\tilde{R}_2^\dagger \tilde{R}_2 \right)^2 + \lambda_3 \left[\text{Tr}(S_3^\dagger S_3) \right]^2 + \lambda'_3 \text{Tr}(S_3^\dagger S_3^\dagger) \text{Tr}(S_3 S_3) + \lambda_{H1} H^\dagger H S_1^\dagger S_1 \\
& + \lambda_{H2} H^\dagger H \tilde{R}_2^\dagger \tilde{R}_2 + \frac{1}{2} \lambda_{H3} H^\dagger H \text{Tr}(S_3^\dagger S_3) + (\lambda_{13} H^\dagger S_3^\dagger H S_1 + \mu_1 \tilde{R}_2^\dagger H S_1^* \\
& + \mu_2 \tilde{R}_2^\dagger S_3^\dagger H + \text{h.c.}),
\end{aligned} \tag{4}$$

where H is the SM Higgs doublet. More general interactions of leptoquarks and SM Higgs can be found in Ref. [72]. After the spontaneous electroweak symmetry breaking, the Higgs field H acquires a vacuum expecting value (VEV) with $\langle H \rangle = v/\sqrt{2}$, $v = 246 \text{ GeV}$. The physical scalar particles include one electric neutral Higgs boson h , three 1/3-charged leptoquarks, two 2/3-charged leptoquarks, and one 4/3-charged leptoquark. In the basis of $\rho^{1/3} \equiv (S_1^{1/3}, \tilde{R}_2^{1/3}, S_3^{1/3})^T$ and $\rho^{2/3} \equiv (\tilde{R}_2^{2/3}, S_3^{2/3})^T$, the mass matrices for the two groups of charged scalar particles are given by

$$M_{1/3}^2 = \begin{pmatrix} m_1^2 + \frac{1}{2} \lambda_{H1} v^2 & \frac{1}{\sqrt{2}} \mu_1 v & -\frac{1}{2} \lambda_{13} v^2 \\ \frac{1}{\sqrt{2}} \mu_1 v & m_2^2 + \frac{1}{2} \lambda_{H2} v^2 & -\frac{1}{\sqrt{2}} \mu_2 v \\ -\frac{1}{2} \lambda_{13} v^2 & -\frac{1}{\sqrt{2}} \mu_2 v & m_3^2 + \frac{1}{2} \lambda_{H3} v^2 \end{pmatrix}, \tag{5}$$

$$M_{2/3}^2 = \begin{pmatrix} m_2^2 + \frac{1}{2} \lambda_{H2} v^2 & \mu_2 v \\ \mu_2 v & m_3^2 + \frac{1}{2} \lambda_{H3} v^2 \end{pmatrix}. \tag{6}$$

After diagonalization of the above mass matrices, we obtain the physical scalar fields: charge-1/3 leptoquarks (ϕ_1, ϕ_2, ϕ_3) and charge-2/3 leptoquarks (ω_1, ω_2) , which satisfy

$$\phi_i = R_{ij}^{1/3} \rho_j^{1/3}, \tag{7}$$

$$\omega_i = R_{ij}^{2/3} \rho_j^{2/3}, \tag{8}$$

where $R^{1/3}$ and $R^{2/3}$ are the corresponding rotation matrices. The rotation matrix $R^{2/3}$ can be parametrized as

$$R^{2/3} = \begin{pmatrix} \cos \alpha & \sin \alpha \\ -\sin \alpha & \cos \alpha \end{pmatrix}, \tag{9}$$

where the mixing angle is given by

$$\tan 2\alpha = \frac{2\mu_2 v}{m_2^2 - m_3^2 + (\lambda_{H2} - \lambda_{H3})v^2/2}. \tag{10}$$

The rotation matrix $R^{1/3}$ need three rotation angles to be parametrized,

$$R^{1/3} = R(\theta_{12})R(\theta_{13})R(\theta_{23}). \tag{11}$$

In the limit where off-diagonal elements are much smaller than the diagonal elements, the mixing angle in the rotation matrix $R^{1/3}$ can be approximatively calculated by

$$\theta_{ij} \simeq \frac{\left(M_{1/3}^2 \right)_{ij}}{\left(M_{1/3}^2 \right)_{ii} - \left(M_{1/3}^2 \right)_{jj}}. \tag{12}$$

The charge-4/3 component $S_3^{4/3}$ has no mixing with other scalar fields and we denote the mass by m_{S_3} . In our analysis of the low energy processes, we assume the leptoquark multiplets to be quasi-degenerate and set the LQ masses as $m_{S_1} = m_{\phi_1}$, $m_{R_2} = m_{\phi_2} \approx m_{\omega_1}$ and $m_{S_3} = m_{\phi_3} \approx m_{\omega_2}$.

B. Neutrino masses

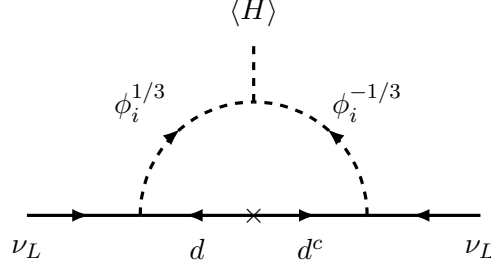


FIG. 1. Feynman diagram of Majorana neutrino masses generation at one-loop level.

In our model, the neutrino masses are induced at one-loop level through the Feynman diagrams as shown in Fig. 1, in which the loop is mediated by the down-type quarks and 1/3-charged leptoquarks. The neutrino mass matrix is given by [67]

$$(\mathcal{M}_\nu)_{\alpha\beta} = \frac{3}{16\pi^2} \sum_{\substack{i=1,2,3 \\ k=d,s,b}} m_k B_0(0, m_k^2, m_{\phi_i}^2) \left\{ R_{i1}^{1/3} R_{i2}^{1/3} \left[(V^T y_{1L})^{k\alpha} y_{2L}^{k\beta} + (V^T y_{1L})^{k\beta} y_{2L}^{k\alpha} \right] \right. \\ \left. + R_{i2}^{1/3} R_{i3}^{1/3} \left[(V^T y_{3L})^{k\alpha} y_{2L}^{k\beta} + (V^T y_{3L})^{k\beta} y_{2L}^{k\alpha} \right] \right\}, \quad (13)$$

where $B_0(0, m_k^2, m_{\phi_i}^2)$ is the Passarino-Veltman function and its finite part is given by

$$B_0(0, m_k^2, m_{\phi_i}^2) = \frac{m_k^2 \log(m_k^2) - m_{\phi_i}^2 \log(m_{\phi_i}^2)}{m_k^2 - m_{\phi_i}^2}. \quad (14)$$

The first term in the bracket of Eq. (13) is associated with the $S_1 - \tilde{R}_2$ combination, while the second term is associated with the $S_3 - \tilde{R}_2$ combination. To simplify the analysis, we consider one term dominates the other. For example, when $S_1 - \tilde{R}_2$ contribution is dominant ($\mu_1 \gg \mu_2, \lambda_{13}v$), the neutrino mass matrix can be written as

$$(\mathcal{M}_\nu)_{\alpha\beta} = (\hat{y}_{1L}^T \Lambda y_{2L} + y_{2L}^T \Lambda^T \hat{y}_{1L})_{\alpha\beta}, \quad (15)$$

where we define $\hat{y}_{1L} \equiv (V^T y_{1L})$ and

$$\Lambda \equiv \begin{pmatrix} \Lambda_d & 0 & 0 \\ 0 & \Lambda_s & 0 \\ 0 & 0 & \Lambda_b \end{pmatrix}, \quad \text{with } \Lambda_k \simeq \frac{3}{32\pi^2} m_k \frac{\sqrt{2}\mu_1 v}{m_{\phi_1}^2 - m_{\phi_2}^2} \log \left(\frac{m_{\phi_1}^2}{m_{\phi_2}^2} \right). \quad (16)$$

Using the method of master parametrization [73, 74], we parametrize the coupling matrices \hat{y}_{1L} and y_{2L} as

$$\hat{y}_{1L} = \frac{1}{\sqrt{2}} \Sigma^{-1/2} W A \hat{D}^{1/2} U^\dagger, \quad (17)$$

$$y_{2L} = \frac{1}{\sqrt{2}} \Sigma^{-1/2} W^* B \hat{D}^{1/2} U^\dagger, \quad (18)$$

where U is the 3×3 unitary neutrino mixing matrix, which brings the neutrino mass matrix to diagonal form by

$$U^T \mathcal{M}_\nu U = \text{diag}(m_1, m_2, m_3). \quad (19)$$

The forms of matrix Σ, W, A, B and \hat{D} depend on the ranks of neutrino mass matrix \mathcal{M}_ν and matrix Λ . Neutrino oscillation data requires that \mathcal{M}_ν should contain two or three non-vanishing eigenvalues. In our numerical analysis of neutrino masses, for simplicity, we neglect the d -quark contribution in neutrino mass loop ($\Lambda_d = 0$) and consider the normal ordering neutrino mass hierarchy with $m_1 = 0$. In this scenario, the ranks of matrices \mathcal{M}_ν and Λ are both 2 and the neutrino mass matrix \mathcal{M}_ν only depends on the second and third columns of couplings \hat{y}_{1L} and y_{2L} . In this case, Σ takes form as $\text{diag}(\Lambda_s, \Lambda_b)$ and \hat{D} takes the form as $\text{diag}(\kappa, m_2, m_3)$, where κ can be arbitrary value, since it can always be absorbed by rescaling relevant elements in matrices A and B . Eq. (17) and Eq. (18) give the elements of second and third columns of couplings \hat{y}_{1L} and y_{2L} . The matrix W is a 2×2 unitary complex matrix that contains 4 real degrees of freedom. The matrices A and B are defined as $A = T C_1$ and $B = (T^T)^{-1} (C_1 C_2 + K C_2)$, where T is an upper-triangular 2×2 complex matrix with positive real values in the diagonal and contains 4 degrees of freedom, K is a 2×2 anti-symmetric complex matrix that contains 2 degrees of freedom. The matrices C_1 and C_2 are given by

$$C_1 = \begin{pmatrix} z_1 & 0 & 0 \\ z_2 & 0 & 0 \end{pmatrix}, \quad C_2 = \begin{pmatrix} -1 & 0 & 0 \\ 0 & 1 & 0 \\ 0 & 0 & 1 \end{pmatrix}, \quad (20)$$

where z_1 and z_2 are two complex numbers that contains 2 degrees of freedom with the condition $z_1^2 + z_2^2 = 0$. The possible values of the second and third columns of matrices \hat{y}_{1L} and y_{2L} can be obtained by scanning these 12 real free parameters.

C. Effective Lagrangians

The tree-level contributions of leptoquarks to the related phenomenologies can be described by the following effective Lagrangians,

$$\mathcal{L}_{\bar{q}q\bar{\ell}\ell} = -\frac{4G_F}{\sqrt{2}} \left[(g_{V,q}^{LL})^{ij,mn} (\bar{q}_L^i \gamma^\mu q_L^j) (\bar{\ell}_L^m \gamma_\mu \ell_L^n) + (g_{V,q}^{RL})^{ij,mn} (\bar{q}_R^i \gamma^\mu q_R^j) (\bar{\ell}_L^m \gamma_\mu \ell_L^n) \right]$$

$$\begin{aligned}
& + (g_{V,q}^{LR})^{ij,mn} (\bar{q}_L^i \gamma^\mu q_L^j) (\bar{\ell}_R^m \gamma_\mu \ell_R^n) + (g_{V,q}^{RR})^{ij,mn} (\bar{q}_R^i \gamma^\mu q_R^j) (\bar{\ell}_R^m \gamma_\mu \ell_R^n) \\
& + (g_{S,q}^{LL})^{ij,mn} (\bar{q}_R^i q_L^j) (\bar{\ell}_R^m \ell_L^n) + (g_{S,q}^{RR})^{ij,mn} (\bar{q}_L^i q_R^j) (\bar{\ell}_L^m \ell_R^n) \\
& + (g_{T,q}^{LL})^{ij,mn} (\bar{q}_R^i \sigma^{\mu\nu} q_L^j) (\bar{\ell}_R^m \sigma_{\mu\nu} \ell_L^n) + (g_{T,q}^{RR})^{ij,mn} (\bar{q}_L^i \sigma^{\mu\nu} q_R^j) (\bar{\ell}_L^m \sigma_{\mu\nu} \ell_R^n) \Big], \quad (21)
\end{aligned}$$

$$\mathcal{L}_{\bar{q}q\bar{\nu}\nu} = \frac{4G_F}{\sqrt{2}} \left[(h_{V,q}^{LL})^{ij,mn} (\bar{q}_L^i \gamma^\mu q_L^j) (\bar{\nu}_L^m \gamma_\mu \nu_L^n) + (h_{V,q}^{RL})^{ij,mn} (\bar{q}_R^i \gamma^\mu q_R^j) (\bar{\nu}_L^m \gamma_\mu \nu_L^n) \right], \quad (22)$$

$$\begin{aligned}
\mathcal{L}_{\bar{u}d\bar{\ell}\nu} = & -\frac{4G_F}{\sqrt{2}} \left[(c_V^{LL})^{ij,mn} (\bar{u}_L^i \gamma^\mu d_L^j) (\bar{\ell}_L^m \gamma_\mu \nu_L^n) + (c_S^{LL})^{ij,mn} (\bar{u}_R^i d_L^j) (\bar{\ell}_R^m \nu_L^n) \right. \\
& \left. + (c_T^{LL})^{ij,mn} (\bar{u}_R^i \sigma^{\mu\nu} d_L^j) (\bar{\ell}_R^m \sigma_{\mu\nu} \nu_L^n) \right] + \text{h.c.} . \quad (23)
\end{aligned}$$

The Wilson coefficients at the leptoquark mass scale are determined by the combinations of Yukawa couplings and summarized in Table I. To analyze the low-energy processes, these Wilson coefficients are needed to RGE run down to the appropriate scale. We take the low-energy scale at the bottom-quark mass ($m_b = 4.18$ GeV) and the Wilson coefficients at the leading logarithm approximation can be calculated by the following form [75–78],

$$C_J(\mu = m_b) = \left[\frac{\alpha_s(m_b)}{\alpha_s(m_t)} \right]^{-\gamma_1^J/\beta_1^{(5)}} \left[\frac{\alpha_s(m_t)}{\alpha_s(m_{\text{LQ}})} \right]^{-\gamma_1^J/\beta_1^{(6)}} C_J(\mu = m_{\text{LQ}}), \quad (24)$$

with the QCD running coefficient $\beta_1^{(n_f)} = (2n_f - 33)/6$, where n_f is the relevant number of quark flavors at the hadronic scale. The coefficients γ_1^J are the anomalous dimension and given by $\gamma_1^V = 0$, $\gamma_1^S = 2$ and $\gamma_1^T = -2/3$. In our numerical analysis, we use the package *Wilson* [79] to calculate the running of Wilson coefficients and obtain the following Wilson coefficient correlations between the two scales,

$$\begin{aligned}
c_V^{LL}(m_b) &= 1.01 c_V^{LL}(m_{\text{LQ}}), \\
\begin{pmatrix} c_S^{LL}(m_b) \\ c_T^{LL}(m_b) \end{pmatrix} &= \begin{pmatrix} 1.64 & -0.275 \\ -3.87 \times 10^{-3} & 0.867 \end{pmatrix} \begin{pmatrix} c_S^{LL}(m_{\text{LQ}}) \\ c_T^{LL}(m_{\text{LQ}}) \end{pmatrix} \quad (25)
\end{aligned}$$

where we have taken the leptoquark masses scale as $m_{\text{LQ}} = 1$ TeV. In the following discussion of the various physical processes, we utilize the *Flavio* package [80] to get the favored region of Wilson coefficients at the leptoquark mass scale.

III. THE FLAVOR ANOMALIES

In this section, we present the observed flavor anomalies between current experimental observations and the SM predictions, and explore how to alleviate these tensions by introducing scalar leptoquarks in our framework.

	S_1	\tilde{R}_2	S_3
$u^i \rightarrow u^j \bar{\ell}^m \ell^n$	$g_{V,u}^{LL} = -(y_{1L})^{im} (y_{1L}^*)^{jn}$ $g_{V,u}^{RR} = -(y_{1R})^{im} (y_{1R}^*)^{jn}$ $g_{S,u}^{LL} = (y_{1R})^{im} (y_{1L}^*)^{jn}$ $g_{S,u}^{RR} = (y_{1L})^{im} (y_{1R}^*)^{jn}$ $g_{T,u}^{LL} = -\frac{1}{4} (y_{1R})^{im} (y_{1L}^*)^{jn}$ $g_{T,u}^{RR} = -\frac{1}{4} (y_{1L})^{im} (y_{1R}^*)^{jn}$		$g_{V,u}^{LL} = -(y_{3L})^{im} (y_{3L}^*)^{jn}$
$d^i \rightarrow d^j \bar{\ell}^m \ell^n$		$g_{V,d}^{RL} = (y_{2L})^{jm} (y_{2L}^*)^{in}$	$g_{V,d}^{LL} = -2(V^T y_{3L})^{im} (V^\dagger y_{3L}^*)^{jn}$
$u^i \rightarrow u^j \bar{\nu}^m \nu^n$			$h_{V,u}^{LL} = 2(y_{3L})^{im} (y_{3L}^*)^{jn}$
$d^i \rightarrow d^j \bar{\nu}^m \nu^n$	$h_{V,d}^{LL} = -(V^T y_{1L})^{im} (V^\dagger y_{1L}^*)^{jn}$	$h_{V,d}^{RL} = -(y_{2L})^{jm} (y_{2L}^*)^{in}$	$h_{V,d}^{LL} = (V^T y_{3L})^{im} (V^\dagger y_{3L}^*)^{jn}$
$d^i \rightarrow u^j \ell^n \bar{\nu}^m$	$c_V^{LL} = (V^T y_{1L})^{im} (y_{1L}^*)^{jn}$ $c_S^{LL} = -(V^T y_{1L})^{im} (y_{1R}^*)^{jn}$ $c_T^{LL} = \frac{1}{4} (V^T y_{1L})^{im} (y_{1R}^*)^{jn}$		$c_V^{LL} = -(V^T y_{3L})^{im} (y_{3L}^*)^{jn}$

TABLE I. The corresponding Wilson coefficients (in units of $v^2/4 m_{LQ}^2$) in Eqs. (21, 22, 23) induced by the leptoquarks at tree level. The matching scale is set at the leptoquark mass scale.

A. R_K and R_{K^*}

The first observed anomalies we consider are the lepton flavor universality violation ratios R_K and R_{K^*} , which are defined as

$$R_K = \frac{\text{Br}(B^+ \rightarrow K^+ \mu^+ \mu^-)}{\text{Br}(B^+ \rightarrow K^+ e^+ e^-)}, \quad R_{K^*} = \frac{\text{Br}(B^0 \rightarrow K^{*0} \mu^+ \mu^-)}{\text{Br}(B^0 \rightarrow K^{*0} e^+ e^-)}. \quad (26)$$

The SM predictions [81, 82] for these two ratios are

$$R_K^{\text{SM}} = 1.0003 \pm 0.0001, \quad R_{K^*}^{\text{SM}} = 1.00 \pm 0.01. \quad (27)$$

The new measurements of R_K and R_{K^*} at low q^2 region [1.1, 6.0] GeV² by LHCb are given by [49, 51]

$$R_K^{\text{LHCb}} = 0.846_{-0.039-0.012}^{+0.042+0.013}, \quad R_{K^*}^{\text{LHCb}} = 0.685_{-0.069}^{+0.113} \pm 0.047, \quad (28)$$

which both give deviation larger than 2.5σ from the SM prediction values. These two processes are determined by the neutral current, $b \rightarrow s \ell^+ \ell^-$. The effective Hamiltonian relevant to our model can be described by [83],

$$\mathcal{H}_{\text{eff}} = -\frac{4G_F}{\sqrt{2}} V_{tb} V_{ts}^* \left[\sum_{X=9,10} (C_X^{\ell\ell} \mathcal{O}_X^{\ell\ell} + C_{X'}^{\ell\ell} \mathcal{O}_{X'}^{\ell\ell}) \right] + \text{h.c.}, \quad (29)$$

where the $C_X^{\ell\ell}$ and $C_{X'}^{\ell\ell}$ denote the Wilson coefficients and $\mathcal{O}_X^{\ell\ell}$ and $\mathcal{O}_{X'}^{\ell\ell}$ are the corresponding effective operators, which take form as

$$\mathcal{O}_9^{\ell\ell} = \frac{e^2}{(4\pi)^2} (\bar{s} \gamma^\mu P_L b) (\bar{\ell} \gamma_\mu \ell), \quad \mathcal{O}_{10}^{\ell\ell} = \frac{e^2}{(4\pi)^2} (\bar{s} \gamma^\mu P_L b) (\bar{\ell} \gamma_\mu \gamma_5 \ell),$$

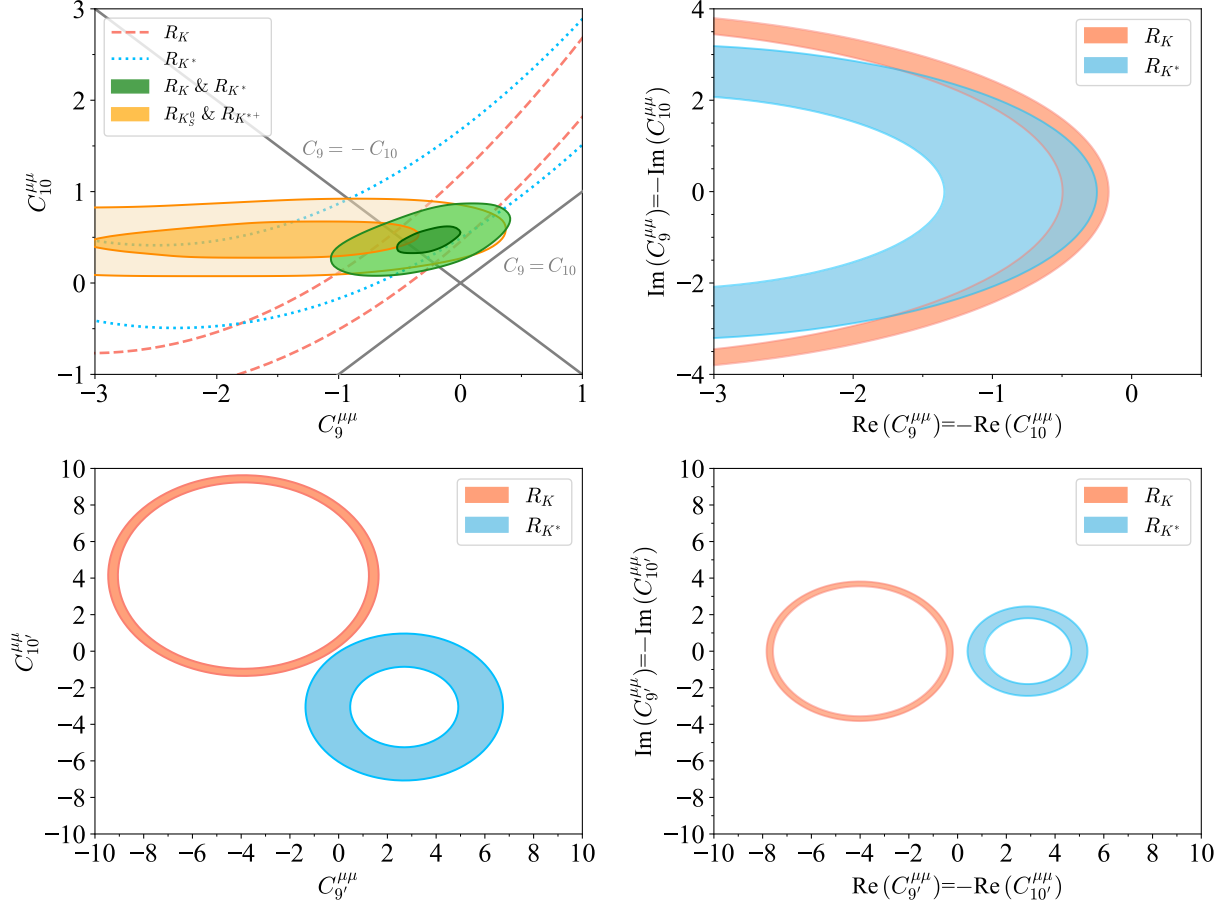


FIG. 2. Contour plot of the fit to R_K and R_{K^*} in the plane of Wilson coefficients at the scale $\mu = 1$ TeV. Upper left panel corresponds to $C_9^{\mu\mu}$ versus $C_{10}^{\mu\mu}$ as real. The dashed orange and dotted blue contours represent the 1σ allowed regions that explain R_K and R_{K^*} respectively. The dark green (yellow) region corresponds to the 1σ allowed region that explains R_K and R_{K^*} ($R_{K_S^0}$ and $R_{K^{*+}}$) simultaneously, while lighter region corresponds to 2σ allowed region. Upper right: The plot corresponds to the complex plane of $C_{9,10}^{\mu\mu}$, with $C_9^{\mu\mu} = -C_{10}^{\mu\mu}$ assumed. The orange and blue regions represent the 1σ allowed regions that explain R_K and R_{K^*} , respectively. Bottom: Left panel shows the fit to $R_{K^{(*)}}$ using $C_{9'}^{\mu\mu}$ and $C_{10'}^{\mu\mu}$ as real parameters, while right one corresponds to the fit using complex parameters with the assumption $C_{9'}^{\mu\mu} = -C_{10'}^{\mu\mu}$. No overlap region indicates that $C_{9'}^{\mu\mu}$ and $C_{10'}^{\mu\mu}$ can not accommodate combined explanation for R_K and R_{K^*} .

$$\mathcal{O}_{9'}^{\ell\ell} = \frac{e^2}{(4\pi)^2} (\bar{s}\gamma^\mu P_R b) (\bar{\ell}\gamma_\mu \ell), \quad \mathcal{O}_{10'}^{\ell\ell} = \frac{e^2}{(4\pi)^2} (\bar{s}\gamma^\mu P_R b) (\bar{\ell}\gamma_\mu \gamma_5 \ell). \quad (30)$$

According to the definition of R_K and R_{K^*} , the anomalies of $R_{K^{(*)}}$ indicate new physics contribution to $C_{9(\prime)}^{ee}$, $C_{10(\prime)}^{ee}$, $C_{9(\prime)}^{\mu\mu}$ and $C_{10(\prime)}^{\mu\mu}$. The solution of R_{K^*} is favored by new physics coupling to muon instead of electron, with the consideration from other observables fit [84–86]. Therefore, we set the new physics contribution related to electron is negligible (i.e., $C_9^{ee} = C_{10}^{ee} \sim 0$), and the new physics contributions to R_K and R_{K^*} come from the $C_9^{\mu\mu}$ and

$C_{10}^{\mu\mu}$ in our framework. We show the fit to $R_{K^{(*)}}$ using $C_{9^{(\prime)},10^{(\prime)}}$ at the scale $\mu = 1$ TeV in Fig. 2. The upper left panel gives favored regions for $C_9^{\mu\mu}$ versus $C_{10}^{\mu\mu}$ as real parameters. We also consider the recent measurements for the ratio $R_{K_S^0}$ and $R_{K^{*+}}$ [87]. Note that we combine the constraint from $B_s \rightarrow \mu\mu$ in the fit. The branching ratio of $B_s \rightarrow \mu\mu$ is measured to be $\text{Br}(B_s \rightarrow \mu\mu)^{\text{exp}} = (2.93 \pm 0.35) \times 10^{-9}$ [88], which is the combined result based on measurements from ATLAS, CMS and LHCb [89–92], while the SM prediction value is $\text{Br}(B_s \rightarrow \mu\mu)^{\text{SM}} = (3.63 \pm 0.13) \times 10^{-9}$ [93]. Taking the relation $C_9^{\mu\mu} = -C_{10}^{\mu\mu}$ given by our model, the best fit point of $R_{K^{(*)}}$ is found at $C_9^{\mu\mu} = -C_{10}^{\mu\mu} = -0.39$, while the best fit point for $R_{K_S^0}$ and $R_{K^{*+}}$ is found at $C_9^{\mu\mu} = -C_{10}^{\mu\mu} = -0.74$. Combining these four experimental ratios and the branching ratio of $B_s \rightarrow \mu\mu$, the best fit point of $C_9^{\mu\mu} = -C_{10}^{\mu\mu}$ is -0.45 . The upper right panel shows the favored region for the complex case with the assumption $C_9^{\mu\mu} = -C_{10}^{\mu\mu}$. The bottom panels present the fit to R_K and R_{K^*} using $C_{9',10'}$ and we find no common solution. Our results are comparable with the global analysis performed in Ref. [94], where some related differential branching ratios and angular observables are included. Relevant analyses are also found in Ref. [95–97].

Leptoquark S_1 doesn't contribute to $b \rightarrow s\ell^+\ell^-$ at tree-level but provides contribution by box-diagrams. However, R_K and R_{K^*} anomalies cannot be fully accommodated with leptoquark S_1 only [55, 98]. In our model, we expect that the contributions to solve R_K and R_{K^*} anomalies come dominantly from leptoquark S_3 . The corresponding Wilson coefficients are given by

$$C_9^{\ell\ell} = -C_{10}^{\ell\ell} = \frac{\pi v^2}{V_{tb}V_{ts}^*\alpha_{\text{em}}} \frac{(V^T y_{3L})^{3\ell} (V^\dagger y_{3L}^*)^{2\ell}}{m_{S_3}^2}. \quad (31)$$

Leptoquark \tilde{R}_2 can also generate contribution to the process $b \rightarrow s\ell^+\ell^-$ at tree-level by $C_{9'}$ and $C_{10'}$ terms. The corresponding Wilson coefficients of \tilde{R}_2 contribution are given by

$$C_{9'}^{\ell\ell} = -C_{10'}^{\ell\ell} = -\frac{\pi v^2}{2V_{tb}V_{ts}^*\alpha_{\text{em}}} \frac{y_{2L}^{2\ell} y_{2L}^{*3\ell}}{m_{\tilde{R}_2}^2}. \quad (32)$$

It is noted that the parameter space to explain R_K is incompatible with R_{K^*} if one only use $C_{9'}$ and $C_{10'}$, as shown in the bottom panel of Fig. 2.

B. R_D and R_{D^*}

The next lepton flavor universality violation observables we consider are R_D and R_{D^*} , which are induced by charged current transitions $b \rightarrow c\ell\bar{\nu}_\ell$ and defined as

$$R_D = \frac{\text{Br}(B \rightarrow D\tau\bar{\nu})}{\text{Br}(B \rightarrow D\ell\bar{\nu})}, \quad R_{D^*} = \frac{\text{Br}(B \rightarrow D^*\tau\bar{\nu})}{\text{Br}(B \rightarrow D^*\ell\bar{\nu})}, \quad (33)$$

where ℓ denotes electron e or muon μ . The predicted values of these two observed quantities in the SM are [99–102]

$$R_D^{\text{SM}} = 0.299 \pm 0.003, \quad R_{D^*}^{\text{SM}} = 0.258 \pm 0.003. \quad (34)$$

These two observables have been measured independently by several collaborations, including Babar [42, 43], Belle [44, 45] and LHCb [48, 103, 104]. The average values by combining these measurements are given by [105]

$$R_D^{\text{exp}} = 0.340 \pm 0.027 \pm 0.013, \quad R_{D^*}^{\text{exp}} = 0.295 \pm 0.011 \pm 0.008, \quad (35)$$

which exceed the SM predictions by 1.4σ and 2.5σ respectively. To confront the leptoquarks contributions with the above experimental data, we consider the following effective Hamiltonian,

$$\begin{aligned} \mathcal{H}_{\text{eff}} = \frac{4G_F}{\sqrt{2}} V_{cb} & \left[g_{V_L} (\bar{c}_L \gamma_\mu b_L) (\bar{\tau}_L \gamma^\mu \nu_L) + g_{S_L} (\bar{c}_R b_L) (\bar{\tau}_R \nu_L) \right. \\ & \left. + g_T (\bar{c}_R \sigma_{\mu\nu} b_L) (\bar{\tau}_R \sigma^{\mu\nu} \nu_L) \right] + \text{h.c.} . \end{aligned} \quad (36)$$

In the Fig. 3, we show the fit of g_{S_L} , g_T and g_{V_L} favored region to explain R_D and R_{D^*} anomalies at the scale of 1 TeV. The upper left panel presents the fit using real parameters g_{S_L} and g_T . With the relation of $g_{S_L} = -4g_T$, which is in our model, the best fit point is $g_{S_L} = -4g_T = 0.12$ and the allowed 1σ range is $g_{S_L} = -4g_T \in [0.08, 0.16]$. If we solely consider the Wilson coefficient g_{V_L} , the best fit point is $g_{V_L} = 0.08(-2.07)$ and the allowed 1σ range is $g_{V_L} \in [0.07, 0.10] \cup [-2.10, -2.05]$. We show the χ^2 values to fit both R_D and R_{D^*} in the upper right panel. We also present the fit result when the coefficients are taken as complex numbers. Comprehensive analyses including the ratio $R_{J/\psi}$, the longitudinal polarization of the $P_\tau(D^*)$ and $F_L^{D^*}$ can be found in Ref. [106–108]. The best fit values in this work agree with theirs in the 1σ allowed range.

In the model, both S_1 and S_3 give contributions to $b \rightarrow c\tau\bar{\nu}$ at tree-level, while \tilde{R}_2 does not. After Fierz transformation to relevant effective Lagrangian, g_{S_L} and g_T have relation $g_{S_L} = -4g_T$. The corresponding Wilson coefficient of S_1 contributions are given by

$$g_{V_L}^\ell = \frac{v^2}{4V_{cb}} \frac{(V^T y_{1L})^{3\ell} y_{1L}^{*23}}{m_{S_1}^2}, \quad (37)$$

$$g_{S_L}^\ell = -4g_T^\ell = -\frac{v^2}{4V_{cb}} \frac{(V^T y_{1L})^{3\ell} y_{1R}^{*23}}{m_{S_1}^2}. \quad (38)$$

The contribution from leptoquark S_3 gives

$$g_{V_L}^\ell = -\frac{v^2}{4V_{cb}} \frac{(V^T y_{3L})^{3\ell} y_{3L}^{*23}}{m_{S_3}^2}. \quad (39)$$

However the contributions of $g_{V_L}^\ell$ from both leptoquarks S_1 and S_3 can not explain the anomalies of $R_{D^{(*)}}$ since its favored parameters space is incompatible with B meson decay process $B \rightarrow K\nu\bar{\nu}$. To explain the anomalies of $R_{D^{(*)}}$, it is required that $y_{1L,3L}^{33} y_{1L,3L}^{23} \sim 0.1$, but the products of couplings are strongly constrained by the process $B \rightarrow K\nu\bar{\nu}$ with $|y_{1L,3L}^{33} y_{1L,3L}^{23}| \lesssim 0.03$. Therefore we focus on the Wilson coefficients $g_{S_L}^\ell$ and g_T^ℓ contribution from the Leptoquark S_1 to explain the anomalies of $R_{D^{(*)}}$.

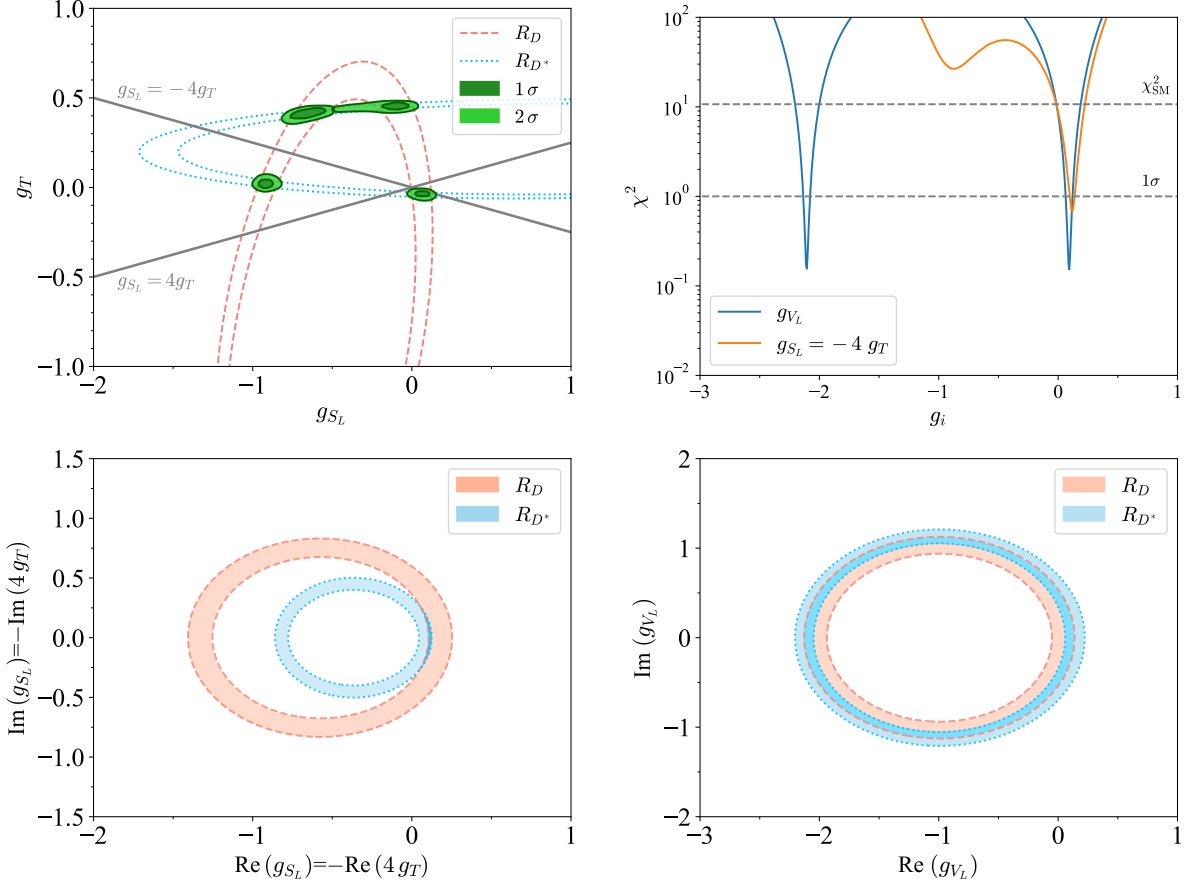


FIG. 3. Upper left: Contour plot of the fit for R_D and R_{D^*} in the plane of g_{S_L} versus g_T at the scale $\mu = 1$ TeV. The dashed orange and dotted blue contours represent the 1σ allowed regions that explain R_D and R_{D^*} , respectively. The dark (light) green region corresponds to the 1σ (2σ) allowed region that explains both simultaneously. Upper right: The χ^2 values to fit both R_D and R_{D^*} when using g_{V_L} and $g_{S_L} = -4g_T$ respectively. Bottom: Two plots correspond to the complex planes of $g_{S_L} = -4g_T$ and g_{V_L} , respectively. The orange and blue regions represent the 1σ allowed region of R_D and R_{D^*} , respectively. The deeper blue region corresponds to the overlap scenario where accommodates combined explanation for R_D and R_{D^*} .

C. The anomalous magnetic moments of charged leptons

The last observable anomalies we consider are the anomalous magnetic moments of charged leptons, including electron and muon, which both exist long-standing discrepancy between the SM predictions and experimental measurements. The recent combined result of Fermilab [41] and BNL [109] increases the tension of muon ($g - 2$), which gives a 4.2σ level deviation from the SM prediction. The precise discrepancy between the SM predictions and experimental values reads [19–41]

$$\Delta a_e = a_e^{\text{exp}} - a_e^{\text{SM}} = -(8.7 \pm 3.6) \times 10^{-13}, \quad (40)$$

$$\Delta a_\mu = a_\mu^{\text{exp}} - a_\mu^{\text{SM}} = (2.51 \pm 0.59) \times 10^{-9}. \quad (41)$$

We start to discuss the contributions to $(g-2)_\ell$ from general scalar Leptoquark interactions, which is described by [68, 110]

$$\mathcal{L}^{F=0} = \bar{q}_i (y_R^{ij} P_R + y_L^{ij} P_L) \ell_j S + \text{h.c.}, \quad (42)$$

$$\mathcal{L}^{|F|=2} = \bar{q}_i^C (y_R'^{ij} P_R + y_L'^{ij} P_L) \ell_j S + \text{h.c.}. \quad (43)$$

Here q^i denotes quark, ℓ denotes charged leptons, S stands for leptoquarks and F is the fermion number. The contributions to $\Delta a_\ell \equiv (g-2)_\ell/2$ from $F=0$ terms are illustrated in Fig. 4 and given by

$$\Delta a_\ell = -\frac{3m_\ell}{8\pi^2 m_S^2} \sum_q \left[m_\ell (|y_R^{q\ell}|^2 + |y_L^{q\ell}|^2) F(x) + m_q \text{Re}(y_L^{*q\ell} y_R^{q\ell}) G(x) \right], \quad (44)$$

where

$$\begin{aligned} F(x) &= Q_S f_S(x) - f_F(x), \\ G(x) &= Q_S g_S(x) - g_F(x), \end{aligned} \quad (45)$$

and the loop functions are calculated by following formulas,

$$\begin{aligned} f_S(x) &= \frac{x+1}{4(1-x)^2} + \frac{x \ln x}{2(1-x)^3}, \\ f_F(x) &= \frac{2+5x-x^2}{12(1-x)^3} + \frac{x \ln x}{2(1-x)^4}, \\ g_S(x) &= \frac{-1}{1-x} - \frac{\ln x}{(1-x)^2}, \\ g_F(x) &= \frac{x-3}{2(1-x)^2} - \frac{\ln x}{(1-x)^3}, \end{aligned} \quad (46)$$

where $x = m_q^2/m_S^2$ and Q_S is the charge of leptoquark S . The $|F|=2$ scalar leptoquarks contribution can be obtained by changing the couplings $y \rightarrow y'$ in Eq. (44). It is noted that the no-chiral scalar leptoquarks which have both left-handed and right-handed couplings to quarks can give a chiral-enhanced contributions to Δa_ℓ by the quark masses. This is revealed by Eq. (44), in which the first term is proportional to the lepton mass, while the second term is proportional to the internal quark mass. Besides, it is worthy to notice that only the second term in Eq. (44) can provide different sign contribution, since the deviation Δa_e and Δa_μ have opposite sign. Thereby among all the scalar leptoquarks, only singlet S_1 or doublet R_2 could provide solution to explain Δa_e and Δa_μ simultaneously. However, the constraint from the branching ratio of $\mu \rightarrow e\gamma$ excludes the one internal quark, such as the top quark, dominating solution [111]. In our model, we choose the scenario that the contributions to Δa_e and Δa_μ come from different quarks. The new contribution is mainly coming from the leptoquark S_1 mediated loop and the contribution to Δa_ℓ is given by

$$\Delta a_\ell \simeq -\sum_q \frac{3m_\ell m_q}{8\pi^2 m_{S_1}^2} \text{Re}(y_{1R}^{*q\ell} y_{1L}^{q\ell}) \left[\frac{7}{6} + \frac{2}{3} \ln x \right]. \quad (47)$$

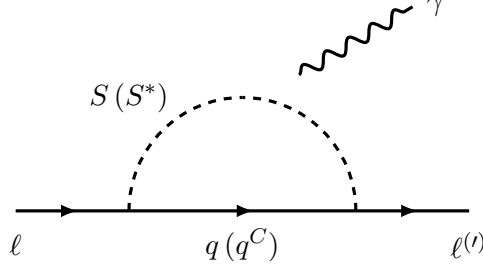


FIG. 4. One-loop diagram contributing to the charged leptons anomalous magnetic moments and the flavor changing process $\ell \rightarrow \ell' \gamma$.

IV. LOW ENERGY CONSTRAINTS

In the previous section, we have discussed the solution to the B -physics anomalies, $R_{K^{(*)}}$ and $R_{D^{(*)}}$, and the anomalous charged lepton magnetic moments, Δa_e and Δa_μ . The model also gives rise to various flavor violating processes and rare meson decays, which are severely constrained by current experiments. In this section, we summarize the most stringent low-energy processes and give the relevant constraints to the leptoquark couplings in the model.

A. $\ell \rightarrow \ell' \gamma$ processes

The lepton flavor violation $\ell \rightarrow \ell' \gamma$ processes, such as $\mu \rightarrow e \gamma$, $\tau \rightarrow e \gamma$ and $\tau \rightarrow \mu \gamma$, can be induced via the one-loop diagrams shown in Fig. 4. The non-chiral leptoquark S_1 contribution to $\ell \rightarrow \ell' \gamma$ processes is enhanced by the quark mass. On the contrary, the chiral leptoquarks \tilde{R}_2 and S_3 induce $\ell \rightarrow \ell' \gamma$ processes without chiral enhancement. The current experimental limits on the lepton flavor violation $\ell \rightarrow \ell' \gamma$ processes are summarized as following [112, 113],

$$\text{Br}(\mu \rightarrow e \gamma) < 4.2 \times 10^{-13}, \quad (48)$$

$$\text{Br}(\tau \rightarrow e \gamma) < 3.3 \times 10^{-8}, \quad (49)$$

$$\text{Br}(\tau \rightarrow \mu \gamma) < 4.4 \times 10^{-8}. \quad (50)$$

The branching ratio of the process $\ell \rightarrow \ell' \gamma$ mediated by the leptoquarks can be calculated by the following formula,

$$\text{Br}(\ell \rightarrow \ell' \gamma) = \frac{\alpha_{\text{em}}(m_\ell^2 - m_{\ell'}^2)^3}{4m_\ell^3 \Gamma(\ell)} \left(|\sigma_R^{\ell\ell'}|^2 + |\sigma_L^{\ell\ell'}|^2 \right), \quad (51)$$

where $\Gamma(\ell)$ is the total decay width of the lepton ℓ and the form factors $\sigma_L^{\ell\ell'}$ and $\sigma_R^{\ell\ell'}$ originating from S_1 , \tilde{R}_2 and S_3 contribution are calculated as

$$\sigma_{L,S_1}^{\ell\ell'} = \frac{3}{16\pi^2 m_{S_1}^2} \sum_{q=u,c,t} \left\{ \left[m_\ell y_{1R}^{q\ell} y_{1R}^{*q\ell'} + m_{\ell'} y_{1L}^{q\ell} y_{1L}^{*q\ell'} \right] \left[\frac{1}{3} f_S(x) - f_F(x) \right] \right\}$$

$$+ m_q (y_{1L}^{q\ell} y_{1R}^{*q\ell'}) \left[\frac{1}{3} g_S(x) - g_F(x) \right] \Big\}, \quad (52)$$

$$\begin{aligned} \sigma_{R,S_1}^{\ell\ell'} = & \frac{3}{16\pi^2 m_{S_1}^2} \sum_{q=u,c,t} \left\{ \left[m_\ell y_{1L}^{q\ell} y_{1L}^{*q\ell'} + m_{\ell'} y_{1R}^{q\ell} y_{1R}^{*q\ell'} \right] \left[\frac{1}{3} f_S(x) - f_F(x) \right] \right. \\ & \left. + m_q (y_{1R}^{q\ell} y_{1L}^{*q\ell'}) \left[\frac{1}{3} g_S(x) - g_F(x) \right] \right\}, \end{aligned} \quad (53)$$

$$\sigma_{L,\tilde{R}_2}^{\ell\ell'} = \frac{3}{16\pi^2 m_{\tilde{R}_2}^2} \sum_{q=d,s,b} m_{\ell'} y_{2L}^{q\ell} y_{2L}^{*q\ell'} \left[\frac{2}{3} f_S(x) - f_F(x) \right], \quad (54)$$

$$\sigma_{R,\tilde{R}_2}^{\ell\ell'} = \frac{3}{16\pi^2 m_{\tilde{R}_2}^2} \sum_{q=d,s,b} m_\ell y_{2L}^{q\ell} y_{2L}^{*q\ell'} \left[\frac{2}{3} f_S(x) - f_F(x) \right], \quad (55)$$

$$\begin{aligned} \sigma_{L,S_3}^{\ell\ell'} = & \frac{3}{16\pi^2 m_{S_3}^2} \left\{ \sum_{q=d,s,b} 2m_{\ell'} (V^T y_{3L})^{q\ell} (V^\dagger y_{3L}^*)^{q\ell'} \left[\frac{4}{3} f_S(x) - f_F(x) \right] \right. \\ & \left. + \sum_{q=u,c,t} m_{\ell'} y_{3L}^{q\ell} y_{3L}^{*q\ell'} \left[\frac{1}{3} f_S(x) - f_F(x) \right] \right\}, \end{aligned} \quad (56)$$

$$\begin{aligned} \sigma_{R,S_3}^{\ell\ell'} = & \frac{3}{16\pi^2 m_{S_3}^2} \left\{ \sum_{q=d,s,b} 2m_\ell (V^T y_{3L})^{q\ell} (V^\dagger y_{3L}^*)^{q\ell'} \left[\frac{4}{3} f_S(x) - f_F(x) \right] \right. \\ & \left. + \sum_{q=u,c,t} m_\ell y_{3L}^{q\ell} y_{3L}^{*q\ell'} \left[\frac{1}{3} f_S(x) - f_F(x) \right] \right\}, \end{aligned} \quad (57)$$

where the loop functions $f_{S,F}(x)$ and $g_{S,F}(x)$ are defined in Eqs. (46). The terms above proportional to m_q arising from the non-chiral leptoquark S_1 give an enhancement and the corresponding couplings are more severely limited. Whereas the chiral leptoquarks \tilde{R}_2 and S_3 only consist of the terms proportional to $m_{\ell(\ell')}$ and get weaker limits. To get the constraints on the couplings, we assume that only the relevant term dominates the contribution. The relevant constraints on the leptoquark Yukawa couplings are summarized in Table II.

B. $\mu - e$ conversion in nuclei

Besides the charged lepton flavor violating radiative decay processes, $\mu - e$ conversion in nuclei is also a rare process providing stringent constraints on the strength of leptoquark interactions. The current experimental search on $\mu - e$ conversion using gold nucleus provides the most stringent upper limits and the upper bound to the branching ratio is set by the SINDRUM experiment as [114]

$$\text{Br}(\mu - e)_{\text{Au}} = \frac{\Gamma(\mu - e)_{\text{Au}}}{\Gamma_{\text{capture}}} < 7 \times 10^{-13}, \quad (58)$$

where the $\Gamma_{\text{capture}} = 8.6 \times 10^{-18}$ GeV denotes the muon capture rate by gold nucleus [115]. The $\mu - e$ conversion rate in nuclei can be calculated by following formula [116, 117]

$$\Gamma(\mu - e) = 2G_F^2 m_\mu^5 \left| \tilde{g}_{LS}^{(p)} S^{(p)} + \tilde{g}_{LS}^{(n)} S^{(n)} + \tilde{g}_{LV}^{(p)} V^{(p)} + \tilde{g}_{LV}^{(n)} V^{(n)} \right|^2 + (L \rightarrow R). \quad (59)$$

Process	Constraints
$\mu \rightarrow e\gamma$	$ y_{1L}^{12}y_{1R}^{*11} , y_{1L}^{*11}y_{1R}^{12} < 3.57 \times 10^{-4} \left(\frac{m_{S_1}}{\text{TeV}}\right)^2$ $ y_{1L}^{22}y_{1R}^{*21} , y_{1L}^{*21}y_{1R}^{22} < 1.29 \times 10^{-6} \left(\frac{m_{S_1}}{\text{TeV}}\right)^2$ $ y_{1L}^{32}y_{1R}^{*31} , y_{1L}^{*31}y_{1R}^{32} < 5.38 \times 10^{-8} \left(\frac{m_{S_1}}{\text{TeV}}\right)^2$ $ y_{1L}^{i2}y_{1L}^{*i1} , y_{1R}^{i2}y_{1R}^{*i1} , y_{3L}^{i2}y_{3L}^{*i1} < 1.31 \times 10^{-3} \left(\frac{m_{S_1/S_3}}{\text{TeV}}\right)^2$ $ (V^T y_{3L})^{i2}(V^\dagger y_{3L}^*)^{i1} < 3.98 \times 10^{-4} \left(\frac{m_{S_3}}{\text{TeV}}\right)^2$
$\tau \rightarrow e\gamma$	$ y_{1L}^{13}y_{1R}^{*11} , y_{1L}^{*11}y_{1R}^{13} < 3.99 \left(\frac{m_{S_1}}{\text{TeV}}\right)^2$ $ y_{1L}^{23}y_{1R}^{*21} , y_{1L}^{*21}y_{1R}^{23} < 1.45 \times 10^{-2} \left(\frac{m_{S_1}}{\text{TeV}}\right)^2$ $ y_{1L}^{33}y_{1R}^{*31} , y_{1L}^{*31}y_{1R}^{33} < 6.02 \times 10^{-4} \left(\frac{m_{S_1}}{\text{TeV}}\right)^2$ $ y_{1L}^{i3}y_{1L}^{*i1} , y_{1R}^{i3}y_{1R}^{*i1} , y_{3L}^{i3}y_{3L}^{*i1} < 0.874 \left(\frac{m_{S_1/S_3}}{\text{TeV}}\right)^2$ $ (V^T y_{3L})^{i3}(V^\dagger y_{3L}^*)^{i1} < 0.240 \left(\frac{m_{S_3}}{\text{TeV}}\right)^2$
$\tau \rightarrow \mu\gamma$	$ y_{1L}^{13}y_{1R}^{*12} , y_{1L}^{*12}y_{1R}^{13} < 4.61 \left(\frac{m_{S_1}}{\text{TeV}}\right)^2$ $ y_{1L}^{23}y_{1R}^{*22} , y_{1L}^{*22}y_{1R}^{23} < 1.67 \times 10^{-2} \left(\frac{m_{S_1}}{\text{TeV}}\right)^2$ $ y_{1L}^{33}y_{1R}^{*32} , y_{1L}^{*32}y_{1R}^{33} < 6.95 \times 10^{-4} \left(\frac{m_{S_1}}{\text{TeV}}\right)^2$ $ y_{1L}^{i3}y_{1L}^{*i2} , y_{1R}^{i3}y_{1R}^{*i2} , y_{3L}^{i3}y_{3L}^{*i2} < 1.01 \left(\frac{m_{S_1/S_3}}{\text{TeV}}\right)^2$ $ (V^T y_{3L})^{i3}(V^\dagger y_{3L}^*)^{i2} < 0.278 \left(\frac{m_{S_3}}{\text{TeV}}\right)^2$
$\mu\text{Au} \rightarrow e\text{Au}$	$ y_{1L}^{12}y_{1L}^{*11} , y_{1R}^{12}y_{1R}^{*11} < 4.20 \times 10^{-6} \left(\frac{m_{S_1}}{\text{TeV}}\right)^2$ $ y_{1L}^{12}y_{1R}^{*11} , y_{1R}^{12}y_{1L}^{*11} < 8.12 \times 10^{-6} \left(\frac{m_{S_1}}{\text{TeV}}\right)^2$ $ y_{2L}^{12}y_{2L}^{*11} < 3.40 \times 10^{-6} \left(\frac{m_{R_2}}{\text{TeV}}\right)^2$ $ y_{3L}^{12}y_{3L}^{*11} < 2.14 \times 10^{-6} \left(\frac{m_{S_3}}{\text{TeV}}\right)^2$ $ (V^T y_{3L})^{12}(V^\dagger y_{3L}^*)^{11} < 1.70 \times 10^{-6} \left(\frac{m_{S_3}}{\text{TeV}}\right)^2$

TABLE II. Upper limits on the leptoquark couplings from the processes $\ell \rightarrow \ell'\gamma$ and $\mu\text{Au} \rightarrow e\text{Au}$.

The overlap integral values of gold nucleus are $S^{(p)} = 0.0523$, $S^{(n)} = 0.0610$, $V^{(p)} = 0.0859$, $V^{(n)} = 0.108$ [116]. With the effective Lagrangian given in Eq. (21), the coupling constants \tilde{g} are defined as

$$\tilde{g}_{LS,RS}^{(p)} = \sum_q G_S^{(q,p)} \frac{1}{2} (g_{S,q}^{LL,RR})^{ii,12}, \quad (60)$$

$$\tilde{g}_{LS,RS}^{(n)} = \sum_q G_S^{(q,n)} \frac{1}{2} (g_{S,q}^{LL,RR})^{ii,12}, \quad (61)$$

$$\tilde{g}_{LV}^{(p)} = [(g_{V,u}^{LL})^{11,12} + (g_{V,u}^{RL})^{11,12}] + \frac{1}{2} [(g_{V,d}^{LL})^{11,12} + (g_{V,d}^{RL})^{11,12}], \quad (62)$$

$$\tilde{g}_{RV}^{(p)} = [(g_{V,u}^{RR})^{11,12} + (g_{V,u}^{LR})^{11,12}] + \frac{1}{2} [(g_{V,d}^{RR})^{11,12} + (g_{V,d}^{LR})^{11,12}], \quad (63)$$

$$\tilde{g}_{LV}^{(n)} = \frac{1}{2} [(g_{V,u}^{LL})^{11,12} + (g_{V,u}^{RL})^{11,12}] + [(g_{V,d}^{LL})^{11,12} + (g_{V,d}^{RL})^{11,12}], \quad (64)$$

$$\tilde{g}_{RV}^{(n)} = \frac{1}{2} [(g_{V,u}^{RR})^{11,12} + (g_{V,u}^{LR})^{11,12}] + [(g_{V,d}^{RR})^{11,12} + (g_{V,d}^{LR})^{11,12}], \quad (65)$$

where the coefficients of scalar operators are $G_S^{u,p} = G_S^{d,n} = 5.1$, $G_S^{d,p} = G_S^{u,n} = 4.3$ and $G_S^{s,p} = G_S^{s,n} = 2.5$ [118]. The bounds on the leptoquark couplings from $\text{Br}(\mu - e)_{\text{Au}}$ are summarized in Table II.

C. Rare meson leptonic decays

Introducing leptoquarks could induce meson rare decay processes. In this subsection, we consider the relevant B_s meson rare leptonic decays that include leptonic conserving decays, $B_s \rightarrow \mu^+ \mu^- / \tau^+ \tau^-$, and leptonic flavor violation decay $B_s \rightarrow \mu^\pm \tau^\mp$. The corresponding 4-fermion operators $\mathcal{O}_{9(\ell)}$, $\mathcal{O}_{10(\ell)}$ are given in the Eq. (30). The recent experimental measurements of these processes are given by [88, 119, 120]

$$\text{Br}(B_s \rightarrow \mu^+ \mu^-) = (2.93 \pm 0.35) \times 10^{-9}, \quad (66)$$

$$\text{Br}(B_s \rightarrow \tau^+ \tau^-) < 6.8 \times 10^{-3}, \quad (67)$$

$$\text{Br}(B_s \rightarrow \mu^\pm \tau^\mp) < 1.4 \times 10^{-5}. \quad (68)$$

Among these processes, only the $B_s \rightarrow \mu^+ \mu^-$ has been observed by the current experiments and the branching ratio agrees with SM prediction value at a level of 4σ , $\text{Br}(B_s \rightarrow \mu\mu)^{\text{SM}} = (3.63 \pm 0.13) \times 10^{-9}$ [93], while the current experiments only give upper bounds for the other two processes. The contribution to the decay width of a neutral meson to two charged leptons $P \rightarrow \ell^+ \ell'^-$ can be written as [121]

$$\begin{aligned} \Gamma_{P \rightarrow \ell^+ \ell'^-} = & \frac{1}{64\pi^3} \frac{G_F^2 \alpha_{\text{em}}^2}{m_P^3} f_P^2 |V_{qj} V_{qi}^*|^2 \lambda_1^{1/2} \lambda_2^{1/2} \\ & \times \left\{ \lambda_1 \cdot \left| (m_\ell - m_{\ell'}) \left(C_9^{ij\ell\ell'} - C_{9'}^{ij\ell\ell'} \right) + \frac{m_P^2}{m_q + m_{q'}} (C_S - C'_S) \right|^2 \right. \\ & \left. + \lambda_2 \cdot \left| (m_\ell + m_{\ell'}) \left(C_{10}^{ij\ell\ell'} - C_{10'}^{ij\ell\ell'} \right) + \frac{m_P^2}{m_q + m_{q'}} (C_P - C'_P) \right|^2 \right\}, \quad (69) \end{aligned}$$

where f_P is the meson decay constant, $\lambda_{1,2} = m_P^2 - (m_\ell \pm m_{\ell'})^2$ and $m_q, m_{q'}$ are the masses of the valence quarks in the pseudoscalar meson P . It is noted that the lepton flavor conserving decay process $P \rightarrow \ell^+ \ell^-$ is independent of Wilson coefficients $C_{9(\ell)}$.

D. Rare meson semi-leptonic decays

The meson rare semi-leptonic decays can be induced at the tree-level by the leptoquarks and present constraints on the corresponding parameters. Here we consider $B \rightarrow K \nu \bar{\nu}$ and $B \rightarrow K^* \nu \bar{\nu}$ processes, related to the $(\bar{q} q \bar{\nu} \nu)$ interactions. The corresponding SM predictions are $\text{Br}(B^0 \rightarrow K^0 \nu \nu) = (4.1 \pm 0.5) \times 10^{-6}$ and $\text{Br}(B^0 \rightarrow K^{*0} \nu \nu) = (9.2 \pm 1.0) \times 10^{-6}$ [122, 123], while the current experimental upper limit bounds are given as 2.6×10^{-5} and 1.8×10^{-5} by

Processes	Constraints on the couplings
$B_s^0 \rightarrow \mu^+ \mu^-$	$y_{2L}^{32} y_{2L}^{*22} \in [-1.1, 1.1] \times 10^{-4} \times \left(\frac{m_{R_2}}{\text{TeV}}\right)^2$ $(V^T y_{3L})^{22} (V^\dagger y_{3L}^*)^{32} \in [-5.8, 5.3] \times 10^{-4} \times \left(\frac{m_{S_3}}{\text{TeV}}\right)^2$
$B_s^0 \rightarrow \tau^+ \tau^-$	$y_{2L}^{33} y_{2L}^{*23} \in [-1.3, 1.3] \times \left(\frac{m_{R_2}}{\text{TeV}}\right)^2$ $(V^T y_{3L})^{23} (V^\dagger y_{3L}^*)^{33} \in [-0.63, 0.63] \times \left(\frac{m_{S_3}}{\text{TeV}}\right)^2$
$B_s^0 \rightarrow \mu^\pm \tau^\mp$	$y_{2L}^{32} y_{2L}^{*23}, y_{2L}^{33} y_{2L}^{*22} \in [-0.080, 0.080] \times \left(\frac{m_{R_2}}{\text{TeV}}\right)^2$ $(V^T y_{3L})^{23} (V^\dagger y_{3L}^*)^{32}, (V^T y_{3L})^{22} (V^\dagger y_{3L}^*)^{33} \in [-0.040, 0.040] \times \left(\frac{m_{S_3}}{\text{TeV}}\right)^2$
$B \rightarrow K \nu \bar{\nu}$	$(V^T y_{1L})^{3i} (V^\dagger y_{1L}^*)^{2j} \in [-0.070, 0.029] \times \left(\frac{m_{S_1}}{\text{TeV}}\right)^2$ $y_{2L}^{3i} y_{2L}^{*2j} \in [-0.032, 0.061] \times \left(\frac{m_{R_2}}{\text{TeV}}\right)^2$ $(V^T y_{3L})^{3i} (V^\dagger y_{3L}^*)^{2j} \in [-0.070, 0.029] \times \left(\frac{m_{S_3}}{\text{TeV}}\right)^2$
$B_s^0 - \bar{B}_s^0$	$(V^T y_{1L})^{2i} (V^\dagger y_{1L}^*)^{3i} \in [-0.14, 0.14] \times \left(\frac{m_{S_1}}{\text{TeV}}\right)^2$ $y_{2L}^{2i} y_{2L}^{*3i} \in [-0.14, 0.14] \times \left(\frac{m_{R_2}}{\text{TeV}}\right)^2$ $(V^T y_{3L})^{2i} (V^\dagger y_{3L}^*)^{3i} \in [-0.061, 0.061] \times \left(\frac{m_{S_3}}{\text{TeV}}\right)^2$
$K^0 - \bar{K}^0$	$(V^T y_{1L})^{2i} (V^\dagger y_{1L}^*)^{1i} \in [-0.026, 0.026] \times \left(\frac{m_{S_1}}{\text{TeV}}\right)^2$ $y_{2L}^{2i} y_{2L}^{*1i} \in [-0.026, 0.026] \times \left(\frac{m_{R_2}}{\text{TeV}}\right)^2$ $(V^T y_{3L})^{2i} (V^\dagger y_{3L}^*)^{1i} \in [-0.013, 0.013] \times \left(\frac{m_{S_3}}{\text{TeV}}\right)^2$

TABLE III. Bounds on the leptoquark couplings from neutral mesons mixing and rare decay processes.

the Belle collaboration [124] respectively. To describe the constraints on new physics from the $B \rightarrow K \nu \bar{\nu}$ and $B \rightarrow K^* \nu \bar{\nu}$ processes, the ratio $R_{K^{(*)}}^{\nu\nu}$ is introduced and defined as

$$R_{K^{(*)}}^{\nu\nu} = \frac{\text{Br}^{\text{SM}+\text{NP}}(B \rightarrow K^{(*)} \nu \bar{\nu})}{\text{Br}^{\text{SM}}(B \rightarrow K^{(*)} \nu \bar{\nu})}. \quad (70)$$

The latest Belle results [124] imply $R_K^{\nu\nu} < 3.9$ and $R_{K^*}^{\nu\nu} < 2.7$. As shown in Table I, the contributions to $B \rightarrow K^{(*)} \nu \bar{\nu}$ from leptoquarks S_1 and S_3 are represented by the Wilson coefficients $h_{V,d}^{LL}$, while by the Wilson coefficient $h_{V,d}^{RL}$ for the case of leptoquark \tilde{R}_2 . If the new physics contribution is dominated by the $h_{V,d}^{LL}$ term, the ratios R_K and R_{K^*} can be calculated by the following formula [122],

$$R_{K^{(*)}}^{\nu\nu} = \frac{2}{3} + \sum_{\nu, \nu'} \frac{1}{3|C_L^{\text{SM}}|^2} \left| \delta^{\nu\nu'} C_L^{\text{SM}} + (h_{V,d}^{LL})^{32; \nu\nu'} \right|^2, \quad (71)$$

where C_L^{SM} describes the SM contribution and the value is $C_L^{\text{SM}} = -6.35$. Note that since the experiments cannot detect the neutrinos in the final state, we need sum over all the flavor. On the other hand, if the new physics contribution is only originated from the $h_{V,d}^{RL}$ term, one has $R_K^{\nu\nu} \neq R_{K^*}^{\nu\nu}$ and the ratios are then presented by

$$R_K^{\nu\nu} = \frac{2}{3} + \sum_{\nu, \nu'} \frac{1}{3|C_L^{\text{SM}}|^2} \left[\delta^{\nu\nu'} C_L^{\text{SM}} + (h_{V,d}^{RL})^{32; \nu\nu'} \right] \left[1 + 2 \frac{\delta^{\nu\nu'} C_L^{\text{SM}} \text{Re}(h_{V,d}^{RL})^{32; \nu\nu'}}{|C_L^{\text{SM}}|^2 + |(h_{V,d}^{RL})^{32; \nu\nu'}|^2} \right], \quad (72)$$

$$R_{K^*}^{\nu\nu} = \frac{2}{3} + \sum_{\nu,\nu'} \frac{1}{3|C_L^{\text{SM}}|^2} \left[\delta^{\nu\nu'} C_L^{\text{SM}} + (h_{V,d}^{RL})^{32;\nu\nu'} \right] \left[1 - 1.34 \frac{\delta^{\nu\nu'} C_L^{\text{SM}} \text{Re}(h_{V,d}^{RL})^{32;\nu\nu'}}{|C_L^{\text{SM}}|^2 + |(h_{V,d}^{RL})^{32;\nu\nu'}|^2} \right]. \quad (73)$$

E. Neutral meson mixing

Leptoquarks can induce neutral meson mixing via box diagrams mediated by leptons and leptoquarks. In this subsection we study the constraints from the $B_s^0 - \bar{B}_s^0$ and $K^0 - \bar{K}^0$ mixing. The related effective Hamiltonian can be described by [125]

$$\mathcal{H}_{\text{eff}} = C_{LL}^{ij} (\bar{d}_L^i \gamma^\mu d_L^j) (\bar{d}_L^i \gamma_\mu d_L^j) + C_{RR}^{ij} (\bar{d}_R^i \gamma^\mu d_R^j) (\bar{d}_R^i \gamma_\mu d_R^j) + C_{LR}^{ij} (\bar{d}_L^i \gamma^\mu d_L^j) (\bar{d}_R^i \gamma_\mu d_R^j), \quad (74)$$

where $i, j = 3, 2$ corresponding to $B_s^0 - \bar{B}_s^0$ mixing and $i, j = 2, 1$ related to $K^0 - \bar{K}^0$ mixing. Mapping the contribution of leptoquarks S_1, \tilde{R}_2 and S_3 , we have the Wilson coefficients at the scale $\mu = m_{\text{LQ}}$ in the following form,

$$S_1 : \quad C_{LL}^{ij} = -\frac{1}{128\pi^2 m_{S_1}^2} \sum_k [(V^T y_{1L})^{ik} (V^\dagger y_{1L}^*)^{jk}]^2, \quad (75)$$

$$\tilde{R}_2 : \quad C_{RR}^{ij} = -\frac{1}{128\pi^2 m_{R_2}^2} \sum_k 2(y_{2L}^{ik} y_{2L}^{*jk})^2, \quad (76)$$

$$S_3 : \quad C_{LL}^{ij} = -\frac{1}{128\pi^2 m_{S_3}^2} \sum_k 5 [(V^T y_{3L})^{ik} (V^\dagger y_{3L}^*)^{jk}]^2. \quad (77)$$

The transition of the Wilson coefficients from $\mu = 1 \text{ TeV}$ to $\mu = m_b$ scale are evaluated by the *Wilson* package [79] and the results are given by

$$C_{LL,RR}^{ij}(\mu = 1 \text{ TeV}) = 0.78 C_{LL,RR}^{ij}(\mu = m_b). \quad (78)$$

The current measurements of the mass differences in $B_s^0 - \bar{B}_s^0$ and $K^0 - \bar{K}^0$ mixing are [126],

$$\Delta m_{B_s}^{\text{exp}} = (17.741 \pm 0.020) \times 10^{12} \text{ sec}^{-1}, \quad (79)$$

$$\Delta m_K^{\text{exp}} = (3.484 \pm 0.0009) \times 10^{10} \text{ sec}^{-1}. \quad (80)$$

For the mass difference $\Delta m_{B_s}^{\text{exp}}$, the SM prediction value is $\Delta m_{B_s}^{\text{SM}} = (18.3 \pm 2.7) \times 10^{12} \text{ sec}^{-1}$ [127–129]. But the SM prediction for the mass difference in $K^0 - \bar{K}^0$ mixing has not been precisely estimated [130, 131]. Thereby in our analysis, we take the new physics contribution to $K^0 - \bar{K}^0$ mixing to be compatible with the experimental value. The bounds on the leptoquarks couplings from neutral meson mixing and rare decay processes are summarized in Table III.

V. NUMERICAL ANALYSIS

In this section, we perform a numerical analysis of the model parameter space to supply a common explanation of B -physics anomalies in $R_{K^{(*)}}$, $R_{D^{(*)}}$ and the charged leptons

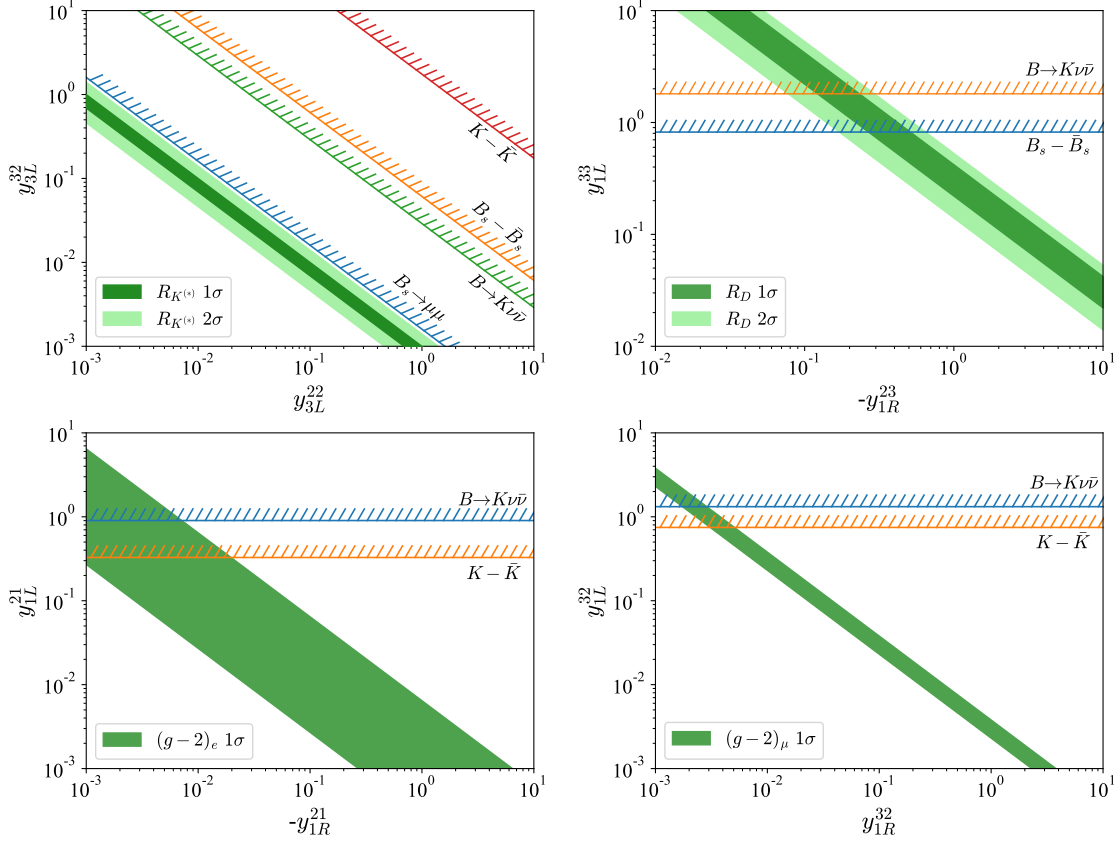


FIG. 5. Allowed regions of the various leptoquark Yukawa couplings obtained from fitting to the corresponding processes. The dark (light) green band represent the 1σ (2σ) allowed regions that explain the corresponding anomalies and the lines denote the constraints from the labelled processes.

anomalous magnetic moment $(g-2)_{e,\mu}$, as well as the neutrino oscillation data. Instead of exploring the entire parameter space, we find the minimal parameters of the model and combine the constraints from the low-energy processes given in the Sec. IV. We fix the components of singlet leptoquark S_1 and triplet leptoquark S_3 mass at 1 TeV ($m_{S_1} = m_{S_3} = 1$ TeV) and fix the components of doublet leptoquark \tilde{R}_2 mass at 2 TeV ($m_{R_2} = 2$ TeV). We use the python package Flavio to obtain the appropriate values of Wilson coefficients that explain the anomalies at the scale of leptoquark masses ($\mu = 1$ TeV) and then analyze the model parameter space.

In order to minimize the number of parameters, we adopt the following form of the Yukawa coupling matrices in the analysis.

$$y_{1R} = \begin{pmatrix} 0 & 0 & 0 \\ y_{1R}^{21} & 0 & y_{1R}^{23} \\ 0 & y_{1R}^{32} & 0 \end{pmatrix}, \quad y_{1L} = \begin{pmatrix} 0 & 0 & 0 \\ y_{1L}^{21} & 0 & y_{1L}^{23} \\ 0 & y_{1L}^{32} & y_{1L}^{33} \end{pmatrix},$$

$$y_{3L} = \begin{pmatrix} 0 & 0 & 0 \\ 0 & y_{3L}^{22} & y_{3L}^{23} \\ y_{3L}^{31} & y_{3L}^{32} & 0 \end{pmatrix}, \quad y_{2L} = \begin{pmatrix} 0 & 0 & 0 \\ y_{2L}^{21} & y_{2L}^{22} & y_{2L}^{23} \\ y_{2L}^{31} & y_{2L}^{32} & y_{2L}^{33} \end{pmatrix}. \quad (81)$$

The coupling combination $(y_{3L}^{22}, y_{3L}^{32})$ can explain the anomalies of R_K and R_{K^*} , while the couplings $(y_{2R}^{33}, y_{2L}^{23})$ can contribute to R_D and R_{D^*} . The couplings $(y_{1R}^{21}, y_{1L}^{21})$ and $(y_{1R}^{32}, y_{1L}^{32})$ give contributions to Δa_e and Δa_μ respectively. The other non-zero couplings are needed to fit the neutrino masses and mixing angles. For a simple illustration, in Fig. 5, we present the allowed parameter space to explain these anomalies and satisfy the relevant processes constraints with taking the coupling as real. Specifically, we provide two concrete benchmark points of the leptoquarks Yukawa couplings. In benchmark point 1, the couplings are chosen as complex number. While for benchmark point 2, we choose the Dirac CP angle in the neutrino mixing matrix as 180° , which is within 1σ allowed range [126] and it is possible to take all the leptoquark Yukawa coupling values as real. The corresponding values of observables for these two benchmark points are summarized in Table IV.

Benchmark point 1:

$$\begin{aligned} y_{1R} &= \begin{pmatrix} 0 & 0 & 0 \\ -0.37 & 0 & -0.70 \\ 0 & 0.054 & 0 \end{pmatrix}, & y_{3L} &= \begin{pmatrix} 0 & 0 & 0 \\ 0 & 0.029 & 0 \\ 0 & 0.023 & 0 \end{pmatrix}, \\ y_{1L} &= \begin{pmatrix} 0 & 0 & 0 \\ 0.012 + 0.016i & 0 & -0.049 - 0.0042i \\ 0 & 0.57 + 0.0082i & 0.59 + 0.052i \end{pmatrix}, \\ y_{2L} &= \begin{pmatrix} 0 & 0 & 0 \\ 0.043 - 0.042i & 0.044 & -0.048 \\ -0.00013 & 0.00038 & 0.00027 \end{pmatrix}. \end{aligned} \quad (82)$$

Benchmark point 2:

$$\begin{aligned} y_{1R} &= \begin{pmatrix} 0 & 0 & 0 \\ -0.014 & 0 & -0.93 \\ 0 & 0.012 & 0 \end{pmatrix}, & y_{1L} &= \begin{pmatrix} 0 & 0 & 0 \\ 0.37 & 0 & 0 \\ 0 & 0.21 & 0.38 \end{pmatrix}, \\ y_{3L} &= \begin{pmatrix} 0 & 0 & 0 \\ 0 & 0.070 & 0.038 \\ 0.0019 & 0.0059 & 0 \end{pmatrix}, & y_{2L} &= \begin{pmatrix} 0 & 0 & 0 \\ -0.015 & -0.0020 & 0.023 \\ 0.0015 & 0.0031 & -0.00078 \end{pmatrix}. \end{aligned} \quad (83)$$

VI. CONCLUSION

In this paper, we have proposed a simple model by extending SM with three TeV-scale scalar leptoquarks S_1 , \tilde{R}_2 and S_3 , where the source of tiny neutrino masses, the lepton flavor

Observables	Allowed range	BP1	BP2
$\Delta m_{21}^2 (10^{-5} \text{eV}^2)$	[6.82, 8.04]	7.44	7.40
$\Delta m_{32}^2 (10^{-3} \text{eV}^2)$	[2.435, 2.598]	2.50	2.51
$\sin^2 \theta_{12}$	[0.269, 0.343]	0.305	0.301
$\sin^2 \theta_{23}$	[0.405, 0.620]	0.569	0.570
$\sin^2 \theta_{13}$	[0.02064, 0.02430]	0.0226	0.0225
$\delta_{\text{CP}}/^\circ$	[169, 246]	194	180
R_K	[0.795, 0.901]	0.808	0.812
R_{K^*}	[0.569, 0.845]	0.794	0.817
$R_{K_S^0}$	[0.48, 0.88]	0.808	0.812
$R_{K^{*+}}$	[0.53, 0.91]	0.825	0.844
R_D	[0.310, 0.370]	0.358	0.351
R_{D^*}	[0.281, 0.309]	0.305	0.292
$\Delta a_e (10^{-13})$	[-12.3, -5.1]	-8.48	-9.89
$\Delta a_\mu (10^{-9})$	[1.93, 3.11]	2.52	2.06
$\text{Br}(\mu \rightarrow e\gamma)$	$< 4.2 \times 10^{-13}$	6.49×10^{-21}	1.04×10^{-17}
$\text{Br}(\tau \rightarrow e\gamma)$	$< 3.3 \times 10^{-8}$	2.98×10^{-18}	6.09×10^{-16}
$\text{Br}(\tau \rightarrow \mu\gamma)$	$< 4.4 \times 10^{-8}$	2.99×10^{-18}	7.82×10^{-16}
$\text{Br}(\mu - e)_{\text{Au}}$	$< 7 \times 10^{-13}$	4.84×10^{-19}	2.62×10^{-15}
$\text{Br}(B_s^0 \rightarrow \mu\mu)$	$[2.58, 3.28] \times 10^{-9}$	2.93×10^{-9}	3.42×10^{-9}
$\text{Br}(B_s^0 \rightarrow \tau\tau)$	$< 6.8 \times 10^{-3}$	7.82×10^{-7}	7.95×10^{-7}
$\text{Br}(B_s^0 \rightarrow \mu\tau)$	$< 1.4 \times 10^{-5}$	2.11×10^{-14}	1.40×10^{-10}
$R_K^{\nu\nu}$	< 3.9	1.3	0.75
$R_{K^*}^{\nu\nu}$	< 2.7	1.4	0.76
$\Delta m_{B_s}^{\text{SM+NP}} / \Delta m_{B_s}^{\text{SM}}$	[0.85, 1.15]	1.03	1.01
$\Delta m_K^{\text{NP}} (10^{10} \text{s}^{-1})$	< 0.95	0.0016	0.52

TABLE IV. Summary of the observable values for the benchmark points.

anomalies in B -meson decays ($R_{K^{(*)}}$, $R_{D^{(*)}}$) and the tension in the charged lepton (electron and muon) anomalous magnetic moments have a common solution. In the model, $R_{K^{(*)}}$ anomalies are resolved by the leptoquark S_3 via the Wilson coefficients $C_{9,10}^{\mu\mu}$. Leptoquark S_1 explains the anomalies of $R_{D^{(*)}}$ through the Wilson coefficients g_{SL}, g_T , as well as the deviations of leptonic magnetic moments $(g-2)_{e,\mu}$ by one-loop level contribution. The small mixing of leptoquarks S_1 with \tilde{R}_2 or \tilde{R}_2 with S_3 can generate tiny neutrino masses. We analyze the parameter space of the leptoquark Yukawa couplings and obtain the corresponding viable region. We study the relevant experimental constraints and conclude there is an appropriate parameter space accommodate to combined explanation for these anomalies and

deviations.

Acknowledgements. This work is supported in part by the National Science Foundation of China (12175082, 11775093) and the Fundamental Research Funds for the Central Universities (CCNU22LJ004).

-
- [1] SUPER-KAMIOKANDE collaboration, *Evidence for oscillation of atmospheric neutrinos*, *Phys. Rev. Lett.* **81** (1998) 1562 [[hep-ex/9807003](#)].
 - [2] SNO collaboration, *Direct evidence for neutrino flavor transformation from neutral current interactions in the Sudbury Neutrino Observatory*, *Phys. Rev. Lett.* **89** (2002) 011301 [[nucl-ex/0204008](#)].
 - [3] KAMLAND collaboration, *First results from KamLAND: Evidence for reactor anti-neutrino disappearance*, *Phys. Rev. Lett.* **90** (2003) 021802 [[hep-ex/0212021](#)].
 - [4] T2K collaboration, *Indication of Electron Neutrino Appearance from an Accelerator-produced Off-axis Muon Neutrino Beam*, *Phys. Rev. Lett.* **107** (2011) 041801 [[1106.2822](#)].
 - [5] E. Ma, *Pathways to naturally small neutrino masses*, *Phys. Rev. Lett.* **81** (1998) 1171 [[hep-ph/9805219](#)].
 - [6] P. Minkowski, $\mu \rightarrow e\gamma$ at a Rate of One Out of 10^9 Muon Decays?, *Phys. Lett. B* **67** (1977) 421.
 - [7] R.N. Mohapatra and G. Senjanovic, *Neutrino Mass and Spontaneous Parity Nonconservation*, *Phys. Rev. Lett.* **44** (1980) 912.
 - [8] M. Gell-Mann, P. Ramond and R. Slansky, *Complex Spinors and Unified Theories*, *Conf. Proc. C* **790927** (1979) 315 [[1306.4669](#)].
 - [9] S.L. Glashow, *The Future of Elementary Particle Physics*, *NATO Sci. Ser. B* **61** (1980) 687.
 - [10] J. Schechter and J.W.F. Valle, *Neutrino Masses in $SU(2) \times U(1)$ Theories*, *Phys. Rev. D* **22** (1980) 2227.
 - [11] R.N. Mohapatra and G. Senjanovic, *Neutrino Masses and Mixings in Gauge Models with Spontaneous Parity Violation*, *Phys. Rev. D* **23** (1981) 165.
 - [12] G. Lazarides, Q. Shafi and C. Wetterich, *Proton Lifetime and Fermion Masses in an $SO(10)$ Model*, *Nucl. Phys. B* **181** (1981) 287.
 - [13] R. Foot, H. Lew, X.G. He and G.C. Joshi, *Seesaw Neutrino Masses Induced by a Triplet of Leptons*, *Z. Phys. C* **44** (1989) 441.
 - [14] A. Zee, *A Theory of Lepton Number Violation, Neutrino Majorana Mass, and Oscillation*, *Phys. Lett. B* **93** (1980) 389.
 - [15] T.P. Cheng and L.-F. Li, *Neutrino Masses, Mixings and Oscillations in $SU(2) \times U(1)$ Models of Electroweak Interactions*, *Phys. Rev. D* **22** (1980) 2860.
 - [16] A. Zee, *Quantum Numbers of Majorana Neutrino Masses*, *Nucl. Phys. B* **264** (1986) 99.

- [17] K.S. Babu, *Model of 'Calculable' Majorana Neutrino Masses*, *Phys. Lett. B* **203** (1988) 132.
- [18] Y. Cai, J. Herrero-García, M.A. Schmidt, A. Vicente and R.R. Volkas, *From the trees to the forest: a review of radiative neutrino mass models*, *Front. in Phys.* **5** (2017) 63 [[1706.08524](#)].
- [19] T. Aoyama, T. Kinoshita and M. Nio, *Revised and Improved Value of the QED Tenth-Order Electron Anomalous Magnetic Moment*, *Phys. Rev. D* **97** (2018) 036001 [[1712.06060](#)].
- [20] A. Keshavarzi, D. Nomura and T. Teubner, *Muon $g - 2$ and $\alpha(M_Z^2)$: a new data-based analysis*, *Phys. Rev.* **D97** (2018) 114025 [[1802.02995](#)].
- [21] M. Davier, A. Hoecker, B. Malaescu and Z. Zhang, *A new evaluation of the hadronic vacuum polarisation contributions to the muon anomalous magnetic moment and to $\alpha(m_Z^2)$* , *Eur. Phys. J.* **C80** (2020) 241 [[1908.00921](#)].
- [22] T. Aoyama et al., *The anomalous magnetic moment of the muon in the Standard Model*, *Phys. Rept.* **887** (2020) 1 [[2006.04822](#)].
- [23] T. Aoyama, M. Hayakawa, T. Kinoshita and M. Nio, *Complete Tenth-Order QED Contribution to the Muon $g - 2$* , *Phys. Rev. Lett.* **109** (2012) 111808 [[1205.5370](#)].
- [24] T. Aoyama, T. Kinoshita and M. Nio, *Theory of the Anomalous Magnetic Moment of the Electron*, *Atoms* **7** (2019) 28.
- [25] A. Czarnecki, W.J. Marciano and A. Vainshtein, *Refinements in electroweak contributions to the muon anomalous magnetic moment*, *Phys. Rev.* **D67** (2003) 073006 [[hep-ph/0212229](#)].
- [26] C. Gnendiger, D. Stöckinger and H. Stöckinger-Kim, *The electroweak contributions to $(g - 2)_\mu$ after the Higgs boson mass measurement*, *Phys. Rev.* **D88** (2013) 053005 [[1306.5546](#)].
- [27] M. Davier, A. Hoecker, B. Malaescu and Z. Zhang, *Reevaluation of the hadronic vacuum polarisation contributions to the Standard Model predictions of the muon $g - 2$ and $\alpha(m_Z^2)$ using newest hadronic cross-section data*, *Eur. Phys. J.* **C77** (2017) 827 [[1706.09436](#)].
- [28] G. Colangelo, M. Hoferichter and P. Stoffer, *Two-pion contribution to hadronic vacuum polarization*, *JHEP* **02** (2019) 006 [[1810.00007](#)].
- [29] M. Hoferichter, B.-L. Hoid and B. Kubis, *Three-pion contribution to hadronic vacuum polarization*, *JHEP* **08** (2019) 137 [[1907.01556](#)].
- [30] A. Keshavarzi, D. Nomura and T. Teubner, *The $g - 2$ of charged leptons, $\alpha(M_Z^2)$ and the hyperfine splitting of muonium*, *Phys. Rev.* **D101** (2020) 014029 [[1911.00367](#)].
- [31] A. Kurz, T. Liu, P. Marquard and M. Steinhauser, *Hadronic contribution to the muon anomalous magnetic moment to next-to-next-to-leading order*, *Phys. Lett.* **B734** (2014) 144 [[1403.6400](#)].
- [32] K. Melnikov and A. Vainshtein, *Hadronic light-by-light scattering contribution to the muon anomalous magnetic moment revisited*, *Phys. Rev.* **D70** (2004) 113006 [[hep-ph/0312226](#)].
- [33] P. Masjuan and P. Sánchez-Puertas, *Pseudoscalar-pole contribution to the $(g_\mu - 2)$: a*

- rational approach, *Phys. Rev.* **D95** (2017) 054026 [[1701.05829](#)].
- [34] G. Colangelo, M. Hoferichter, M. Procura and P. Stoffer, *Dispersion relation for hadronic light-by-light scattering: two-pion contributions*, *JHEP* **04** (2017) 161 [[1702.07347](#)].
- [35] M. Hoferichter, B.-L. Hoid, B. Kubis, S. Leupold and S.P. Schneider, *Dispersion relation for hadronic light-by-light scattering: pion pole*, *JHEP* **10** (2018) 141 [[1808.04823](#)].
- [36] A. Gérardin, H.B. Meyer and A. Nyffeler, *Lattice calculation of the pion transition form factor with $N_f = 2 + 1$ Wilson quarks*, *Phys. Rev.* **D100** (2019) 034520 [[1903.09471](#)].
- [37] J. Bijnens, N. Hermansson-Truedsson and A. Rodríguez-Sánchez, *Short-distance constraints for the HLbL contribution to the muon anomalous magnetic moment*, *Phys. Lett.* **B798** (2019) 134994 [[1908.03331](#)].
- [38] G. Colangelo, F. Hagelstein, M. Hoferichter, L. Laub and P. Stoffer, *Longitudinal short-distance constraints for the hadronic light-by-light contribution to $(g - 2)_\mu$ with large- N_c Regge models*, *JHEP* **03** (2020) 101 [[1910.13432](#)].
- [39] T. Blum, N. Christ, M. Hayakawa, T. Izubuchi, L. Jin, C. Jung et al., *The hadronic light-by-light scattering contribution to the muon anomalous magnetic moment from lattice QCD*, *Phys. Rev. Lett.* **124** (2020) 132002 [[1911.08123](#)].
- [40] G. Colangelo, M. Hoferichter, A. Nyffeler, M. Passera and P. Stoffer, *Remarks on higher-order hadronic corrections to the muon $g - 2$* , *Phys. Lett.* **B735** (2014) 90 [[1403.7512](#)].
- [41] MUON G-2 collaboration, *Measurement of the Positive Muon Anomalous Magnetic Moment to 0.46 ppm*, *Phys. Rev. Lett.* **126** (2021) 141801 [[2104.03281](#)].
- [42] BABAR collaboration, *Evidence for an excess of $\bar{B} \rightarrow D^{(*)}\tau^-\bar{\nu}_\tau$ decays*, *Phys. Rev. Lett.* **109** (2012) 101802 [[1205.5442](#)].
- [43] BABAR collaboration, *Measurement of an Excess of $\bar{B} \rightarrow D^{(*)}\tau^-\bar{\nu}_\tau$ Decays and Implications for Charged Higgs Bosons*, *Phys. Rev. D* **88** (2013) 072012 [[1303.0571](#)].
- [44] BELLE collaboration, *Measurement of the branching ratio of $\bar{B} \rightarrow D^{(*)}\tau^-\bar{\nu}_\tau$ relative to $\bar{B} \rightarrow D^{(*)}\ell^-\bar{\nu}_\ell$ decays with hadronic tagging at Belle*, *Phys. Rev. D* **92** (2015) 072014 [[1507.03233](#)].
- [45] BELLE collaboration, *Measurement of the τ lepton polarization and $R(D^*)$ in the decay $\bar{B} \rightarrow D^*\tau^-\bar{\nu}_\tau$* , *Phys. Rev. Lett.* **118** (2017) 211801 [[1612.00529](#)].
- [46] BELLE collaboration, *Measurement of the branching ratio of $\bar{B}^0 \rightarrow D^{*+}\tau^-\bar{\nu}_\tau$ relative to $\bar{B}^0 \rightarrow D^{*+}\ell^-\bar{\nu}_\ell$ decays with a semileptonic tagging method*, in *51st Rencontres de Moriond on EW Interactions and Unified Theories*, 3, 2016 [[1603.06711](#)].
- [47] LHCb collaboration, *Measurement of the ratio of branching fractions $\mathcal{B}(B_c^+ \rightarrow J/\psi\tau^+\nu_\tau)/\mathcal{B}(B_c^+ \rightarrow J/\psi\mu^+\nu_\mu)$* , *Phys. Rev. Lett.* **120** (2018) 121801 [[1711.05623](#)].
- [48] LHCb collaboration, *Measurement of the ratio of the $B^0 \rightarrow D^{*-}\tau^+\nu_\tau$ and $B^0 \rightarrow D^{*-}\mu^+\nu_\mu$ branching fractions using three-prong τ -lepton decays*, *Phys. Rev. Lett.* **120** (2018) 171802

- [1708.08856].
- [49] LHCb collaboration, *Search for lepton-universality violation in $B^+ \rightarrow K^+ \ell^+ \ell^-$ decays*, *Phys. Rev. Lett.* **122** (2019) 191801 [[1903.09252](#)].
- [50] LHCb collaboration, *Test of lepton universality with $B^0 \rightarrow K^{*0} \ell^+ \ell^-$ decays*, *JHEP* **08** (2017) 055 [[1705.05802](#)].
- [51] LHCb collaboration, *Test of lepton universality in beauty-quark decays*, *Nature Phys.* **18** (2022) 277 [[2103.11769](#)].
- [52] I. Doršner, S. Fajfer, A. Greljo, J.F. Kamenik and N. Košnik, *Physics of leptoquarks in precision experiments and at particle colliders*, *Phys. Rept.* **641** (2016) 1 [[1603.04993](#)].
- [53] A. Crivellin, C. Greub, D. Müller and F. Saturnino, *Scalar Leptoquarks in Leptonic Processes*, *JHEP* **02** (2021) 182 [[2010.06593](#)].
- [54] A. Carvunis, A. Crivellin, D. Guadagnoli and S. Gangal, *The Forward-Backward Asymmetry in $B \rightarrow D^* \ell \nu$: One more hint for Scalar Leptoquarks?*, *Phys. Rev. D* **105** (2022) L031701 [[2106.09610](#)].
- [55] A. Angelescu, D. Bečirević, D.A. Faroughy and O. Sumensari, *Closing the window on single leptoquark solutions to the B -physics anomalies*, *JHEP* **10** (2018) 183 [[1808.08179](#)].
- [56] I. Bigaran, J. Gargalionis and R.R. Volkas, *A near-minimal leptoquark model for reconciling flavour anomalies and generating radiative neutrino masses*, *JHEP* **10** (2019) 106 [[1906.01870](#)].
- [57] S. Saad, *Combined explanations of $(g-2)_\mu$, $R_{D^{(*)}}$, $R_{K^{(*)}}$ anomalies in a two-loop radiative neutrino mass model*, *Phys. Rev. D* **102** (2020) 015019 [[2005.04352](#)].
- [58] V. Gherardi, D. Marzocca and E. Venturini, *Low-energy phenomenology of scalar leptoquarks at one-loop accuracy*, *JHEP* **01** (2021) 138 [[2008.09548](#)].
- [59] A. Greljo, P. Stangl and A.E. Thomsen, *A model of muon anomalies*, *Phys. Lett. B* **820** (2021) 136554 [[2103.13991](#)].
- [60] H.M. Lee, *Leptoquark option for B -meson anomalies and leptonic signatures*, *Phys. Rev. D* **104** (2021) 015007 [[2104.02982](#)].
- [61] A. Bhaskar, A.A. Madathil, T. Mandal and S. Mitra, *Combined explanation of W -mass, muon $g-2$, $R_{K^{(*)}}$ and $R_{D^{(*)}}$ anomalies in a singlet-triplet scalar leptoquark model*, [2204.09031](#).
- [62] C.-H. Chen, T. Nomura and H. Okada, *Explanation of $B \rightarrow K^{(*)} \ell^+ \ell^-$ and muon $g-2$, and implications at the LHC*, *Phys. Rev. D* **94** (2016) 115005 [[1607.04857](#)].
- [63] S. Saad and A. Thapa, *Common origin of neutrino masses and $R_{D^{(*)}}$, $R_{K^{(*)}}$ anomalies*, *Phys. Rev. D* **102** (2020) 015014 [[2004.07880](#)].
- [64] K.S. Babu, P.S.B. Dev, S. Jana and A. Thapa, *Unified framework for B -anomalies, muon $g-2$ and neutrino masses*, *JHEP* **03** (2021) 179 [[2009.01771](#)].
- [65] I. Doršner, S. Fajfer and S. Saad, *$\mu \rightarrow e \gamma$ selecting scalar leptoquark solutions for the $(g-2)_{e,\mu}$ puzzles*, *Phys. Rev. D* **102** (2020) 075007 [[2006.11624](#)].

- [66] I. Bigaran and R.R. Volkas, *Getting chirality right: Single scalar leptoquark solutions to the $(g-2)_{e,\mu}$ puzzle*, *Phys. Rev. D* **102** (2020) 075037 [[2002.12544](#)].
- [67] D. Aristizabal Sierra, M. Hirsch and S.G. Kovalenko, *Leptoquarks: Neutrino masses and accelerator phenomenology*, *Phys. Rev. D* **77** (2008) 055011 [[0710.5699](#)].
- [68] I. Doršner, S. Fajfer and N. Košnik, *Leptoquark mechanism of neutrino masses within the grand unification framework*, *Eur. Phys. J. C* **77** (2017) 417 [[1701.08322](#)].
- [69] J. Julio, S. Saad and A. Thapa, *A flavor-inspired radiative neutrino mass model*, *JHEP* **08** (2022) 270 [[2202.10479](#)].
- [70] J. Julio, S. Saad and A. Thapa, *Marriage between neutrino mass and flavor anomalies*, *Phys. Rev. D* **106** (2022) 055003 [[2203.15499](#)].
- [71] T.A. Chowdhury and S. Saad, *Leptoquark-vectorlike quark model for the CDF m_W , $(g-2)_\mu$, $R_K^{(*)}$ anomalies, and neutrino masses*, *Phys. Rev. D* **106** (2022) 055017 [[2205.03917](#)].
- [72] I. Doršner, S. Fajfer and O. Sumensari, *Triple-leptoquark interactions for tree- and loop-level proton decays*, *JHEP* **05** (2022) 183 [[2202.08287](#)].
- [73] I. Cordero-Carrión, M. Hirsch and A. Vicente, *Master Majorana neutrino mass parametrization*, *Phys. Rev. D* **99** (2019) 075019 [[1812.03896](#)].
- [74] I. Cordero-Carrión, M. Hirsch and A. Vicente, *General parametrization of Majorana neutrino mass models*, *Phys. Rev. D* **101** (2020) 075032 [[1912.08858](#)].
- [75] K.G. Chetyrkin, *Quark mass anomalous dimension to $O(\alpha_s^4)$* , *Phys. Lett. B* **404** (1997) 161 [[hep-ph/9703278](#)].
- [76] J.A. Gracey, *Three loop \overline{MS} tensor current anomalous dimension in QCD*, *Phys. Lett. B* **488** (2000) 175 [[hep-ph/0007171](#)].
- [77] I. Doršner, S. Fajfer, N. Košnik and I. Nišandžić, *Minimally flavored colored scalar in $\bar{B} \rightarrow D^{(*)}\tau\bar{\nu}$ and the mass matrices constraints*, *JHEP* **11** (2013) 084 [[1306.6493](#)].
- [78] G. Hiller, D. Loose and K. Schönwald, *Leptoquark Flavor Patterns & B Decay Anomalies*, *JHEP* **12** (2016) 027 [[1609.08895](#)].
- [79] J. Aebischer, J. Kumar and D.M. Straub, *Wilson: a Python package for the running and matching of Wilson coefficients above and below the electroweak scale*, *Eur. Phys. J. C* **78** (2018) 1026 [[1804.05033](#)].
- [80] D.M. Straub, *flavio: a Python package for flavour and precision phenomenology in the Standard Model and beyond*, [1810.08132](#).
- [81] C. Bobeth, G. Hiller and G. Piranishvili, *Angular distributions of $\bar{B} \rightarrow \bar{K}\ell^+\ell^-$ decays*, *JHEP* **12** (2007) 040 [[0709.4174](#)].
- [82] M. Bordone, G. Isidori and A. Pattori, *On the Standard Model predictions for R_K and R_{K^*}* , *Eur. Phys. J. C* **76** (2016) 440 [[1605.07633](#)].
- [83] G. Buchalla, A.J. Buras and M.E. Lautenbacher, *Weak decays beyond leading logarithms*, *Rev. Mod. Phys.* **68** (1996) 1125 [[hep-ph/9512380](#)].
- [84] B. Capdevila, A. Crivellin, S. Descotes-Genon, J. Matias and J. Virto, *Patterns of New*

- Physics in $b \rightarrow s\ell^+\ell^-$ transitions in the light of recent data*, *JHEP* **01** (2018) 093 [[1704.05340](#)].
- [85] T. Hurth, F. Mahmoudi, D. Martinez Santos and S. Neshatpour, *Lepton nonuniversality in exclusive $b \rightarrow s\ell\ell$ decays*, *Phys. Rev. D* **96** (2017) 095034 [[1705.06274](#)].
- [86] J. Aebischer, W. Altmannshofer, D. Guadagnoli, M. Reboud, P. Stangl and D.M. Straub, *B-decay discrepancies after Moriond 2019*, *Eur. Phys. J. C* **80** (2020) 252 [[1903.10434](#)].
- [87] LHCb collaboration, *Tests of lepton universality using $B^0 \rightarrow K_S^0 \ell^+ \ell^-$ and $B^+ \rightarrow K^{*+} \ell^+ \ell^-$ decays*, *Phys. Rev. Lett.* **128** (2022) 191802 [[2110.09501](#)].
- [88] L.-S. Geng, B. Grinstein, S. Jäger, S.-Y. Li, J. Martin Camalich and R.-X. Shi, *Implications of new evidence for lepton-universality violation in $b \rightarrow s\ell + \ell^-$ decays*, *Phys. Rev. D* **104** (2021) 035029 [[2103.12738](#)].
- [89] ATLAS collaboration, *Study of the rare decays of B_s^0 and B^0 mesons into muon pairs using data collected during 2015 and 2016 with the ATLAS detector*, *JHEP* **04** (2019) 098 [[1812.03017](#)].
- [90] CMS collaboration, *Measurement of properties of $B_s^0 \rightarrow \mu^+ \mu^-$ decays and search for $B^0 \rightarrow \mu^+ \mu^-$ with the CMS experiment*, *JHEP* **04** (2020) 188 [[1910.12127](#)].
- [91] LHCb collaboration, *Measurement of the $B_s^0 \rightarrow \mu^+ \mu^-$ decay properties and search for the $B^0 \rightarrow \mu^+ \mu^-$ and $B_s^0 \rightarrow \mu^+ \mu^- \gamma$ decays*, *Phys. Rev. D* **105** (2022) 012010 [[2108.09283](#)].
- [92] LHCb collaboration, *Analysis of Neutral B-Meson Decays into Two Muons*, *Phys. Rev. Lett.* **128** (2022) 041801 [[2108.09284](#)].
- [93] M. Beneke, C. Bobeth and R. Szafron, *Power-enhanced leading-logarithmic QED corrections to $B_q \rightarrow \mu^+ \mu^-$* , *JHEP* **10** (2019) 232 [[1908.07011](#)].
- [94] A.K. Alok, N.R.S. Chundawat, S. Gangal and D. Kumar, *A global analysis of $b \rightarrow s\ell\ell$ data in heavy and light Z' models*, [2203.13217](#).
- [95] D. Bečirević, S. Fajfer and N. Košnik, *Lepton flavor nonuniversality in $b \rightarrow s\ell^+\ell^-$ processes*, *Phys. Rev. D* **92** (2015) 014016 [[1503.09024](#)].
- [96] A. Carvunis, F. Dettori, S. Gangal, D. Guadagnoli and C. Normand, *On the effective lifetime of $B_s \rightarrow \mu\mu\gamma$* , *JHEP* **12** (2021) 078 [[2102.13390](#)].
- [97] W. Altmannshofer and P. Stangl, *New physics in rare B decays after Moriond 2021*, *Eur. Phys. J. C* **81** (2021) 952 [[2103.13370](#)].
- [98] D. Bečirević, N. Košnik, O. Sumensari and R. Zukanovich Funchal, *Palatable Leptoquark Scenarios for Lepton Flavor Violation in Exclusive $b \rightarrow s\ell_1\ell_2$ modes*, *JHEP* **11** (2016) 035 [[1608.07583](#)].
- [99] D. Bigi and P. Gambino, *Revisiting $B \rightarrow D\ell\nu$* , *Phys. Rev. D* **94** (2016) 094008 [[1606.08030](#)].
- [100] F.U. Bernlochner, Z. Ligeti, M. Papucci and D.J. Robinson, *Combined analysis of semileptonic B decays to D and D^* : $R(D^{(*)})$, $|V_{cb}|$, and new physics*, *Phys. Rev. D* **95** (2017) 115008 [[1703.05330](#)].

- [101] S. Jaiswal, S. Nandi and S.K. Patra, *Extraction of $|V_{cb}|$ from $B \rightarrow D^{(*)} \ell \nu_\ell$ and the Standard Model predictions of $R(D^{(*)})$* , *JHEP* **12** (2017) 060 [[1707.09977](#)].
- [102] D. Bigi, P. Gambino and S. Schacht, *$R(D^*)$, $|V_{cb}|$, and the Heavy Quark Symmetry relations between form factors*, *JHEP* **11** (2017) 061 [[1707.09509](#)].
- [103] LHCb collaboration, *Measurement of the ratio of branching fractions $\mathcal{B}(\bar{B}^0 \rightarrow D^{*+} \tau^- \bar{\nu}_\tau) / \mathcal{B}(\bar{B}^0 \rightarrow D^{*+} \mu^- \bar{\nu}_\mu)$* , *Phys. Rev. Lett.* **115** (2015) 111803 [[1506.08614](#)].
- [104] LHCb collaboration, *Test of Lepton Flavor Universality by the measurement of the $B^0 \rightarrow D^{*-} \tau^+ \nu_\tau$ branching fraction using three-prong τ decays*, *Phys. Rev. D* **97** (2018) 072013 [[1711.02505](#)].
- [105] HFLAV collaboration, *Averages of b -hadron, c -hadron, and τ -lepton properties as of 2018*, *Eur. Phys. J. C* **81** (2021) 226 [[1909.12524](#)].
- [106] C. Murgui, A. Peñuelas, M. Jung and A. Pich, *Global fit to $b \rightarrow c \tau \nu$ transitions*, *JHEP* **09** (2019) 103 [[1904.09311](#)].
- [107] R.-X. Shi, L.-S. Geng, B. Grinstein, S. Jäger and J. Martin Camalich, *Revisiting the new-physics interpretation of the $b \rightarrow c \tau \nu$ data*, *JHEP* **12** (2019) 065 [[1905.08498](#)].
- [108] K. Cheung, Z.-R. Huang, H.-D. Li, C.-D. Lü, Y.-N. Mao and R.-Y. Tang, *Revisit to the $b \rightarrow c \tau \nu$ transition: In and beyond the SM*, *Nucl. Phys. B* **965** (2021) 115354 [[2002.07272](#)].
- [109] MUON G-2 collaboration, *Final Report of the Muon E821 Anomalous Magnetic Moment Measurement at BNL*, *Phys. Rev. D* **73** (2006) 072003 [[hep-ex/0602035](#)].
- [110] K.-m. Cheung, *Muon anomalous magnetic moment and leptoquark solutions*, *Phys. Rev. D* **64** (2001) 033001 [[hep-ph/0102238](#)].
- [111] A. Crivellin, M. Hoferichter and P. Schmidt-Wellenburg, *Combined explanations of $(g-2)_{\mu,e}$ and implications for a large muon EDM*, *Phys. Rev. D* **98** (2018) 113002 [[1807.11484](#)].
- [112] MEG collaboration, *Search for the lepton flavour violating decay $\mu^+ \rightarrow e^+ \gamma$ with the full dataset of the MEG experiment*, *Eur. Phys. J. C* **76** (2016) 434 [[1605.05081](#)].
- [113] BABAR collaboration, *Searches for Lepton Flavor Violation in the Decays $\tau^\pm \rightarrow e^\pm \gamma$ and $\tau^\pm \rightarrow \mu^\pm \gamma$* , *Phys. Rev. Lett.* **104** (2010) 021802 [[0908.2381](#)].
- [114] SINDRUM II collaboration, *A Search for muon to electron conversion in muonic gold*, *Eur. Phys. J. C* **47** (2006) 337.
- [115] T. Suzuki, D.F. Measday and J.P. Roalsvig, *Total Nuclear Capture Rates for Negative Muons*, *Phys. Rev. C* **35** (1987) 2212.
- [116] R. Kitano, M. Koike and Y. Okada, *Detailed calculation of lepton flavor violating muon electron conversion rate for various nuclei*, *Phys. Rev. D* **66** (2002) 096002 [[hep-ph/0203110](#)].
- [117] E. Arganda, M.J. Herrero and A.M. Teixeira, *μ - e conversion in nuclei within the CMSSM seesaw: Universality versus non-universality*, *JHEP* **10** (2007) 104 [[0707.2955](#)].
- [118] T.S. Kosmas, S. Kovalenko and I. Schmidt, *Nuclear muon- e - conversion in strange quark*

- sea, *Phys. Lett. B* **511** (2001) 203 [[hep-ph/0102101](#)].
- [119] LHCb collaboration, *Search for the decays $B_s^0 \rightarrow \tau^+\tau^-$ and $B^0 \rightarrow \tau^+\tau^-$* , *Phys. Rev. Lett.* **118** (2017) 251802 [[1703.02508](#)].
 - [120] LHCb collaboration, *Search for the lepton-flavour-violating decays $B_s^0 \rightarrow \tau^\pm\mu^\mp$ and $B^0 \rightarrow \tau^\pm\mu^\mp$* , *Phys. Rev. Lett.* **123** (2019) 211801 [[1905.06614](#)].
 - [121] D. Bečirević, O. Sumensari and R. Zukanovich Funchal, *Lepton flavor violation in exclusive $b \rightarrow s$ decays*, *Eur. Phys. J. C* **76** (2016) 134 [[1602.00881](#)].
 - [122] A.J. Buras, J. Girrbach-Noe, C. Niehoff and D.M. Straub, *$B \rightarrow K^{(*)}\nu\bar{\nu}$ decays in the Standard Model and beyond*, *JHEP* **02** (2015) 184 [[1409.4557](#)].
 - [123] W. Altmannshofer, A.J. Buras, D.M. Straub and M. Wick, *New strategies for New Physics search in $B \rightarrow K^*\nu\bar{\nu}$, $B \rightarrow K\nu\bar{\nu}$ and $B \rightarrow X_s\nu\bar{\nu}$ decays*, *JHEP* **04** (2009) 022 [[0902.0160](#)].
 - [124] BELLE collaboration, *Search for $B \rightarrow h\nu\bar{\nu}$ decays with semileptonic tagging at Belle*, *Phys. Rev. D* **96** (2017) 091101 [[1702.03224](#)].
 - [125] C. Bobeth and A.J. Buras, *Leptoquarks meet ε'/ε and rare Kaon processes*, *JHEP* **02** (2018) 101 [[1712.01295](#)].
 - [126] PARTICLE DATA GROUP collaboration, *Review of Particle Physics*, *PTEP* **2020** (2020) 083C01.
 - [127] M. Artuso, G. Borissov and A. Lenz, *CP violation in the B_s^0 system*, *Rev. Mod. Phys.* **88** (2016) 045002 [[1511.09466](#)].
 - [128] FERMILAB LATTICE, MILC collaboration, *$B_{(s)}^0$ -mixing matrix elements from lattice QCD for the Standard Model and beyond*, *Phys. Rev. D* **93** (2016) 113016 [[1602.03560](#)].
 - [129] T. Jubb, M. Kirk, A. Lenz and G. Tetlalmatzi-Xolocotzi, *On the ultimate precision of meson mixing observables*, *Nucl. Phys. B* **915** (2017) 431 [[1603.07770](#)].
 - [130] J. Brod and M. Gorbahn, *Next-to-Next-to-Leading-Order Charm-Quark Contribution to the CP Violation Parameter ϵ_K and ΔM_K* , *Phys. Rev. Lett.* **108** (2012) 121801 [[1108.2036](#)].
 - [131] A.J. Buras, J.-M. Gérard and W.A. Bardeen, *Large N Approach to Kaon Decays and Mixing 28 Years Later: $\Delta I = 1/2$ Rule, \hat{B}_K and ΔM_K* , *Eur. Phys. J. C* **74** (2014) 2871 [[1401.1385](#)].